GEOCHEMICAL INVESTIGATION OF THE ROLE OF KEROGEN IN THE RETENTION OF HYDROCARBONS BY ORGANIC-RICH SHALES

A Thesis

Presented to

the Faculty of the Department of Earth and Atmospheric Sciences

University of Houston

In Partial Fulfillment

of the Requirements for the Degree

Masters of Science

By

Gregory E. Sills

December 2014

GEOCHEMICAL INVESTIGATION OF THE ROLE OF KEROGEN IN THE RETENTION OF HYDROCARBONS BY ORGANIC-RICH SHALES

_____

Gregory E. Sills

APPROVED:

_____

Dr. K.K. Bissada, Chairman

_____

Dr. Regina Capuano, Co-Chair

_____

Dr. Ian Evans

_____

Dr. Amy Kelly

Shell Oil Company

_____

Dean Dan E. Wells, College of Natural Sciences and Mathematics

ACKNOWLEDGEMENTS

I would like to thank my advisor, Dr. K.K. (Adry) Bissada, for his invaluable help and guidance throughout the extent of my graduate studies. I would also like to thank my committee members, Dr. Regina Capuano, Dr. Ian Evans, and Dr. Amy Kelly, for their advice and support. Additional thanks go to Dr. Joe Curiale for his assistance with this project. I am very grateful to the Center for Petroleum Geochemistry at the University of Houston for funding my research and for providing me with samples and analytical facilities to conduct this research. Additional thanks go to Ewa Szymczyk, Mike Darnell, Denet Pernia, Maria Gutierrez, and Bryan Gunawan for their assistance in the laboratory. I am most grateful for the support of my family and friends throughout this endeavor.

GEOCHEMICAL INVESTIGATION OF THE ROLE OF KEROGEN IN THE RETENTION OF HYDROCARBONS BY ORGANIC-RICH SHALES

An Abstract of a Thesis

Presented to

the Faculty of the Department of Earth and Atmospheric Sciences

University of Houston

In Partial Fulfillment

of the Requirements for the Degree

Masters of Science

By

Gregory E. Sills

December 2014

ABSTRACT

Modern production technology has made it economically feasible to exploit source rocks as unconventional hydrocarbon resources. Because the resource magnitude depends on hydrocarbon retention in these rocks, understanding and quantifying their hydrocarbon retention capacity is critical for profitable exploitation. Although hydrocarbon retention in organic-rich shales is strongly influenced by fluid/rock interaction, it is not entirely clear whether this is due to hydrocarbon/kerogen or hydrocarbon/mineral interactions.

The objective of this research was to determine the relative importance of hydrocarbon/kerogen vs. hydrocarbon/mineral interactions in the retention phenomenon. One approach to this question is through measuring heats of adsorption (ΔH_a) for the interactions of hydrocarbons with kerogen versus whole-rock. Previous research demonstrated that ΔH_a values for gases on solid adsorbents can be measured by gas-solid chromatography. No study has used this method to quantify hydrocarbon adsorption on kerogen. In this study, a simple system was investigated. The interaction of ethane, propane, n-butane, and i-butane with kerogen isolated from a thermally-immature Green River shale was determined using the chromatographic method. Additionally, ΔH_a values were determined for the interaction of ethane and propane with the whole shale.

ΔH_a values for ethane, propane and n-butane on the kerogen were determined to be -1.76, -2.23, and -4.13 kcal/mol, respectively. The ΔH_a values for ethane and propane on the whole shale were quite similar, measuring -1.40 and -2.32 kcal/mol. The ΔH_a

value for i-butane/kerogen interaction measured only -1.14 kcal/mol. All ΔH_a values are relatively low, suggesting there is no site-specific chemical interaction between the hydrocarbon components and the adsorbents.

ΔH_a values increase with the size of the n-alkanes, and are similar for interactions with the kerogen as with the whole shale. The ΔH_a value measured for i-butane on the kerogen is lower than the ΔH_a value determined for n-butane on the same adsorbent, which can be attributed to the larger molecular diameter of i-butane. These observations suggest that the interactions are controlled primarily by dispersion forces between the organic molecules and the kerogen structure. For this system, the hydrocarbon adsorption potential of the shale is influenced predominantly by adsorption on the kerogen, and not on the matrix minerals.

Table of Contents

Chapter 1: Introduction

1.1. Introduction

Recent advances in hydrocarbon production technologies (horizontal drilling, multi-stage fracking, and state-of-the-art proppants) have made it economically feasible to produce natural gas from previously un-exploitable organic-rich shale reservoirs (Speight, 2013). These extremely low-permeability reservoirs can have very large resource potentials, with shale plays in the United States estimated to contain 600-1100 trillion-cubic-feet (tcf) of gas (EIA, 2011; USGS, 2013a,b; USGS, 2014). Organic-rich shales are often the source rocks of the hydrocarbon gas that they retain. The identification of economically producible zones in these source rocks is difficult due to their diffuse continuous nature, and the absence of focused migration into structural highs that can be mapped by conventional seismic methods.

To obtain accurate gas-in-place reserve estimates and to predict the potential production yield from organic-rich shales, it is necessary to estimate not only their hydrocarbon generation potential and the volume of hydrocarbons they have already expelled into conventional reservoirs, but also the volume of hydrocarbons they retained in the rocks. To develop practical means for assessing hydrocarbon retention, it is necessary to understand how hydrocarbons are stored and retained in these source rocks. Although hydrocarbon retention in organic-rich shales is controlled principally by fluid/rock interaction, it is not entirely clear whether this is due to hydrocarbon/kerogen or hydrocarbon/mineral interactions. It has been suggested that kerogen plays a significant role in shale-gas storage, yet research on hydrocarbon retention in gas-shale kerogen has been limited (Ross and Bustin, 2009; Zhang et al., 2012).

The main objective of this research is to investigate the relative importance of kerogen versus the inorganic matrix in the retention of hydrocarbons by organic-rich shales. To address this objective within the limited time frame for this project, a set of simple experiments were conducted to measure the physicochemical interaction energies between one type of kerogen and a series of single gaseous hydrocarbons on the one hand, and between the whole-rock that contains this kerogen and the same series of gaseous hydrocarbons on the other hand. These experiments provide a better understanding of the physics behind the interaction of hydrocarbons with organic/inorganic surfaces, and can be used as a means to aid in the future development of models of hydrocarbon retention in organic-rich shales.

The rock and kerogen samples used in these experiments consisted of a whole-rock Green River shale and a kerogen isolated from that shale. A brief outline of the rock preparation and subsequent analytical steps undertaken is provided below; a more detailed description of the procedures is given in Chapter 4 of this manuscript.

The whole-rock shale sample was crushed and ground to a particle size of 40-60 mesh (250-400 microns). Kerogen was chemically isolated from the ground shale, and powdered with a mortar and pestle. Bitumen was removed from the kerogen and shale samples via solvent extraction. After bitumen removal, the kerogen and shale were placed in a vacuum-oven overnight at 80°C to remove residual solvent. Total organic carbon analysis was done on the un-extracted and extracted shale to determine organic richness. Ash-content analysis was done on the extracted kerogen to assess kerogen purity. X-ray diffraction was conducted on the extracted shale and kerogen to determine the shale

mineralogy, and to identify any inorganic contaminants in the kerogen. Organic elemental analysis for carbon, hydrogen, nitrogen, and oxygen (CHNO) was done on the extracted kerogen. Analyses were conducted on a Perkin-Elmer 2400 Elemental Analyzer fitted with an oxygen accessory kit. An aliquot of the extracted shale and an aliquot of the corresponding kerogen concentrate were individually packed into two (2) two-foot, 1/4" O.D. columns fabricated out of chromatographic-grade copper tubing.

Gas-chromatographic retention times for ethane (C2) and propane (C3) on the shale-packed column, and retention times for ethane (C2), propane (C3), i-butane (i-C4), and n-butane (n-C4) on the kerogen-packed column, were determined at multiple temperatures using a Hewlett-Packard 5890 series gas-chromatograph. The chromatographic method was used to calculate the energy of adsorption for the interaction of the light hydrocarbon components with the kerogen and whole-rock from the recorded retention times of the mobile-phase gases.

Chapter 2: Background

To appreciate the implications of the current research, it is necessary to first understand the controls on hydrocarbon retention in shale reservoirs. This chapter provides a brief background on organic-rich shale reservoirs, how hydrocarbon gas might be retained in these reservoirs, and the prevailing concepts on the main controls on the retention process.

2.1. Organic-rich shale reservoirs

Organic-rich shales are fine-grained, impermeable rocks that have relatively high organic matter contents. These shales can contain large volumes of retained hydrocarbon fluids, and are often both the source and the reservoir for the hydrocarbons they contain (Jarvie et al., 2007). Hydrocarbon reservoirs are categorized as being either conventional or unconventional. This classification is based on the reservoir permeability and hydrocarbon transmissibility mechanisms (Sondergeld et al., 2010; Speight, 2013) (**Figure 2.1**). Exploitation of organic-rich shales is of the unconventional type.

Conventional hydrocarbon reservoirs are porous, permeable, and discrete geologic structures in which hydrocarbons accumulate following focused, buoyancy-driven migration of the hydrocarbons from the source rock intervals. Hydrocarbons are stored in these reservoirs as density stratified accumulations in structural and stratigraphic traps, where they can be produced easily due to the natural permeability of the reservoir rocks.

In contrast, unconventional hydrocarbon reservoirs are porous yet impermeable rocks that contain continuous accumulations of hydrocarbons trapped in the rock pore-space. These reservoirs can retain large quantities of oil and gas, but the irregular

distribution of hydrocarbon-rich zones complicates resource-volume estimation and makes the identification of favorable drilling sites extremely difficult.

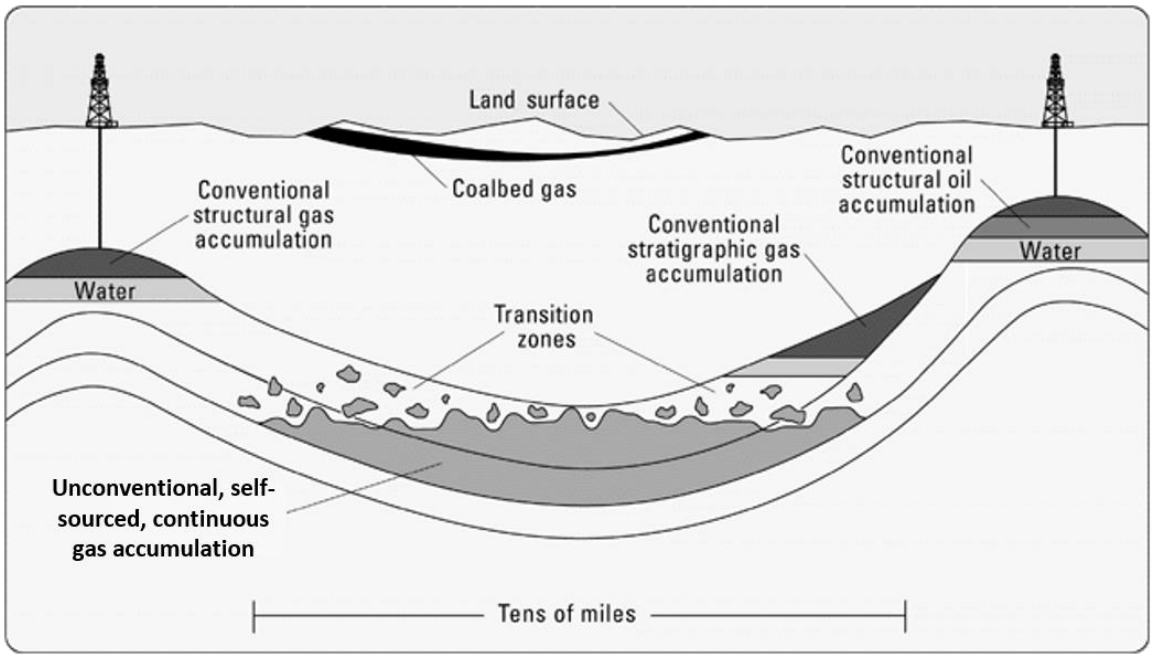

Figure 2.1. Schematic showing the different types of hydrocarbon accumulations, (figure modified from Schenk and Pollastro, 2002).

Conventional vertical drilling is an ineffective practice for commercial production of hydrocarbon-rich zones. Identification of hydrocarbon-rich zones is complicated by the limited knowledge of the extent of hydrocarbon retention subsequent to the normal expulsion phase of the petroleum system's life-cycle (Sondergeld et al., 2010).

The insoluble organic matter fraction (kerogen) of organic-rich shales is suggested to have a significant influence on the storage and retention of hydrocarbons by the shales, but the specific role of organic matter in these processes is not clear (Ross and Bustin, 2009; Rexer et al., 2013). The majority of studies that have measured hydrocarbon adsorption on organic matter relied on coal, carbon powders, or carbon

models as analogues to micro-porous organic matter (Aranovich and Donohue, 1995; Himeno et al., 2005; Rybolt et al., 2006; Rybolt et al., 2008; Yang et al., 2009; Qiu et al., 2012; Xia and Tang, 2012). These types of analogues may not be truly representative of a kerogen and could interact with hydrocarbons differently as a result. Additionally, the majority of data on hydrocarbon retention by kerogen are derived from assumption-based flow modeling, whole-rock diffusion experiments, and whole-rock desorption experiments (Stainforth and Reinders, 1990; Thomas and Clouse, 1990a, 1990b; Zhang et al., 2012). To quantify the role that kerogen has in the retention of hydrocarbons by organic-rich shales, direct measurements of hydrocarbon retention on a pure kerogen must be made. The following section provides a definition of kerogen, and discusses the characteristics of kerogen that could impact the retention of hydrocarbons by organic-rich shales.

2.2. Kerogen

Kerogen is the insoluble organic matter from which hydrocarbons are generated, and comprises the majority of organic matter in organic-rich shales (Demaison and Moore, 1980; Durand, 1980; Vandenbroucke and Largeau, 2007). **Figure 2.2** shows the general composition of organic matter in sedimentary rocks. Kerogen can classified into three types based on the depositional environment of the organic matter, kerogen maceral content, elemental composition, and the type of hydrocarbons that the kerogen can generate (Durand and Espitalié, 1973; Vandenbroucke and Largeau, 2007). Type I, or sapropelic kerogen, is composed of marine- or lacustrine-sourced lipid-rich amorphous

algal remains, is highly aliphatic, and is oil-prone. Type I kerogen has a high initial hydrogen/carbon (H/C) atomic ratio and a low oxygen/carbon (O/C) atomic ratio.

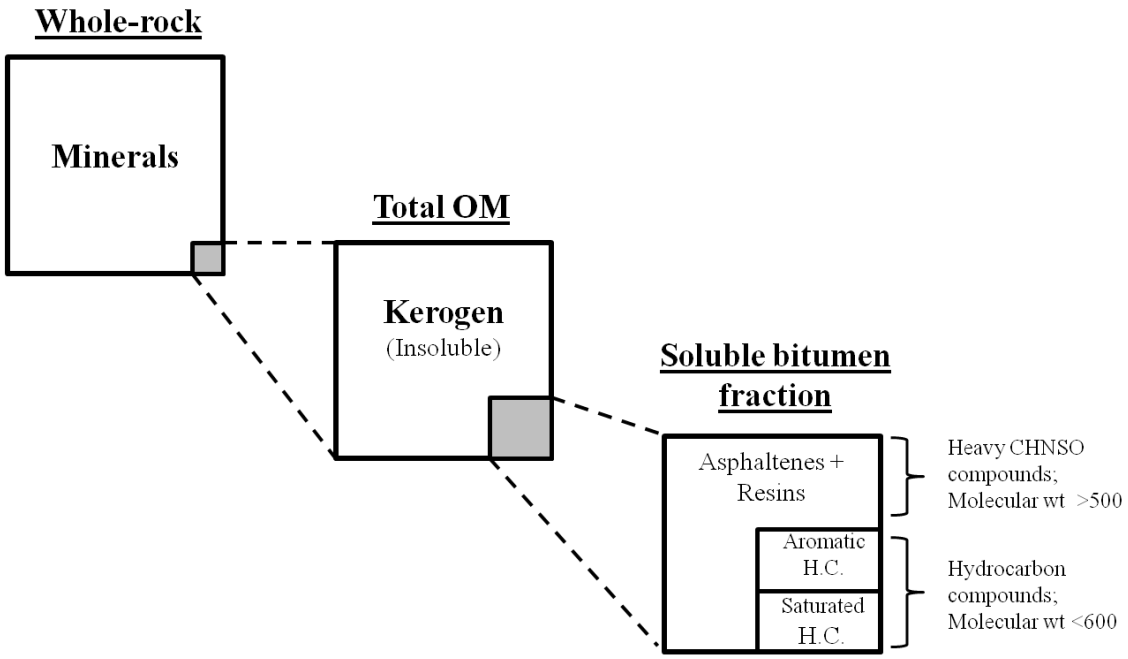

Figure 2.2. Composition of organic matter in typical sedimentary rocks, adapted from Tissot and Welte (1978).

Type II, or exinitic/mixed kerogen, is composed of both marine/lacustrine-sourced amorphous OM and terrestrial-sourced structured OM. Type II kerogen can have both aliphatic and aromatic structural components, and is oil- and gas-prone. Type II kerogen has high H/C ratios and low O/C ratios. Type III, or humic kerogen, is composed of terrestrial-plant-derived lignitic and cellulosic OM, is highly aromatic, and is gas-prone. Type III kerogen has a low initial hydrogen content and high oxygen/carbon (O/C) atomic ratio.

Kerogen can be isolated from sedimentary rocks via physical and chemical separation methods (Forsman and Hunt, 1958; Saxby, 1970; Hitchon et al., 1976; Durand

and Nicaise, 1980; Ibrahimov and Bissada, 2010). Geochemical characterization of isolated kerogen can provide information on the hydrocarbon generation potential of a parent-shale. As the conversion of kerogen to hydrocarbons is dependent on temperature, geochemical determination of a kerogen's thermal history can be used to determine whether or not a parent source rock has generated hydrocarbons. Kerogen H/C and O/C ratios can be plotted on modified van Krevelen diagrams to evaluate kerogen origin and thermal evolution (Durand and Espitalié, 1973; Tissot et al., 1974). A typical van Krevelen diagram is shown in **Figure 2.3**.

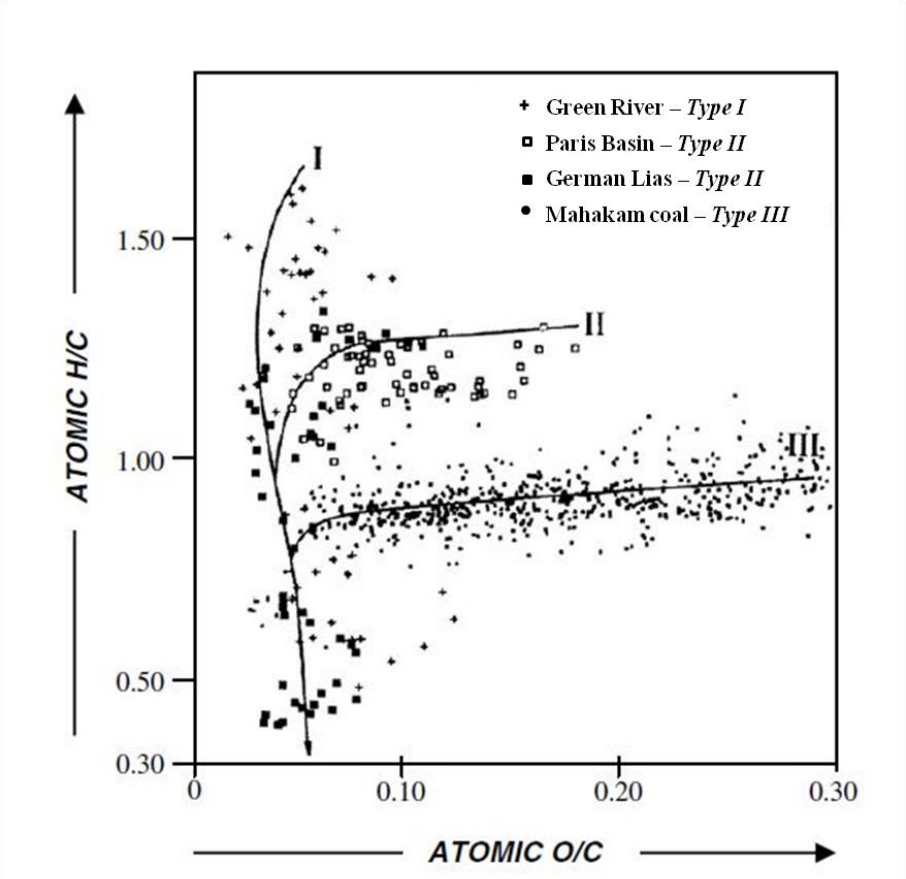

Figure 2.3. Typical van Krevelen diagram, modified from Vandenbroucke and Largeau, 2007.

2.3. Hydrocarbon generation, storage, and retention by shale reservoirs

The processes by which hydrocarbons are generated, stored, and retained in shale reservoirs are all directly related to, or influenced by, the ability of the shale to adsorb hydrocarbons. In order to develop means for estimating the fraction of adsorbed hydrocarbons, it is necessary to first understand the processes by which hydrocarbons are generated, stored, and retained in these reservoirs.

The generation potential of source rocks is primarily determined by the type and amount of kerogen in the rock. As a source-shale is buried, the kerogen contained within the rock is heated and converted to hydrocarbon fluids. Type I source rocks will primarily generate oil, while Type III source rocks will primarily generate gas; Type II source rocks will generate both of oil and gas. When a critical amount of hydrocarbons is generated that exceeds the storage capacity of the source-shale, the rock fractures and hydrocarbons migrate out of the shale along the fracture paths. Some of the generated oil and gas is retained in the pore-space, and on the surfaces of the shale kerogen and mineral matrix, and is not expelled from the source rock. These retained hydrocarbons are the primary target of unconventional oil- and gas-shale exploration and production endeavors.

The hydrocarbon storage capacity of shale reservoirs is primarily dependent on the porosity of the shale; i.e., the amount of space available within the shale for hydrocarbons to accumulate. It is proposed that hydrocarbon gas is stored in organic-rich shale reservoirs as three fractions: (1) as a free fluid in pores and fractures, (2) dissolved in oil or water, and (3) sorbed on the shale's organic matter and matrix minerals (Jarvie et

al., 2007; Jenkins and Boyer, 2008; Zhang et al., 2012; USGS, 2013a). The amount of free-gas and dissolved gas in shale reservoirs is relatively easy to predict, as these fractions are the main component of conventional gas accumulations; methods for quantifying the amount of hydrocarbons stored as a free or dissolved gas have been developed accordingly (Sondergeld et al., 2010). Sorbed gas is unique to unconventional shale reservoirs, and includes gas adsorbed to the surfaces of the shale, as well as absorbed within the shale's internal crystal lattice structure. In this research, only the adsorbed fraction was considered (Gregg and Sing, 1991; Ross and Bustin, 2009). Hydrocarbon adsorption by organic-rich shales is a consequence of chemical and physical interactions between adsorbate hydrocarbon molecules and the adsorbent surfaces of the shale kerogen and inorganic minerals. Quantification of the volume of adsorbed hydrocarbons in unconventional shales is complicated because of the multiple chemical and physical factors that can influence the adsorption process; the chemistry behind the adsorption process is detailed in Chapter 3. However, some relationships can be made between the storage and retention capacity of unconventional shales for hydrocarbons, and the fraction of adsorbed hydrocarbons that these shales contain.

2.4. Controls on hydrocarbon retention by organic-rich shales

2.4.1. Adsorption of hydrocarbons by shales

Hydrocarbon retention in shale reservoirs is influenced mainly by the permeability of the shale, but is also a function of the amount of adsorbed gas on the shale minerals and shale kerogen. Adsorption is just one mechanism by which hydrocarbons are retained in organic-rich shales, but it has been suggested that adsorption

has a strong control on the total volume of retained hydrocarbons in these shales. Jarvie et al. (2007) demonstrated that the degree of gas adsorption in self-sourced shales can influence the amount and type of hydrocarbons that are expelled and subsequently retained in these reservoirs. Heavier hydrocarbon molecules (C4+) will adsorb much more strongly to the surfaces of the shale kerogen and matrix minerals than will light hydrocarbon components (C1-C4). As such, estimates of the relative strength of the interaction between hydrocarbons and the organic/inorganic shale components can be used to help estimate the composition and relative volume of retained gas resources in a shale reservoir. The general composition of natural gas, and its significance for hydrocarbon retention, is discussed in the following sub-section.

2.4.2. Hydrocarbon composition

Natural gas is usually composed of a mixture of hydrocarbon and non-hydrocarbon components. Non-hydrocarbons are molecules composed of carbon and hydrogen, as well as any amount of nitrogen, sulfur, and/or oxygen (NSOs). NSO compounds exhibit different retention behavior than do pure hydrocarbon gases, so knowing the bulk composition of natural gas is necessary for accurate predictions of retained gas volumes. **Table 1** lists the common components of bulk natural gas. Higher proportions of C_{2+} hydrocarbons and non-hydrocarbon components in a gas will usually lead to a greater degree of gas retention in reservoirs. Greater volumes of retained gas in a reservoir essentially limit the amount of gas that can be economically produced, so it is important to know the general composition of contained gas before a particular shale reservoir is produced.

Table 1. Common components of natural gas, with compound names, chemical formulae, and average percent volume of total gas composition shown. (From Speight, 2013).

Compound	Formula	Volume (%)
Methane	CH_4	>85
Ethane	C_2H_6	3 - 8
Propane	C_3H_8	1 - 5
Butane	C_4H_{10}	1 - 2
Pentane*	C_5H_{12}	1 - 5
Carbon dioxide	CO_2	1 - 2
Hydrogen sulfide	H_2S	1 - 2
Nitrogen	N_2	1 - 5
Helium	He	<0.5
Pentane: pentane plus higher weight hydrocarbons, including benzene and toluene*		

The relative concentration of hydrocarbon and non-hydrocarbon components in shale gas is dependent on the type, origin, and thermal maturity of the shale organic matter; these organic matter characteristics, and subsequently gas composition, can vary considerably between different shale formations. The thermal history of gas-bearing shales is also important, as shale gas becomes increasingly methane-rich at higher thermal maturity levels due to the secondary cracking of shale bitumen (Seewald et al., 1998). Due to the large variability in gas composition between different shale gas reservoirs, data derived from experiments on shale gas mixtures are usually only applicable to the shale from which they were sourced. In order to obtain data that is applicable to multiple gas-shales, the retention behavior of individual pure gas components can be studied, and the relative contribution of each can be quantified.

The molecular structure of natural gas hydrocarbons, i.e., the size, shape, and chemical composition of the molecules, can also influence the degree of gas retention in organic-rich shales. Saturated hydrocarbons, or alkanes, have the simplest structure of all hydrocarbon compounds; these molecules have either straight-chain (n-paraffins), branched (iso-paraffins), or cyclic (napthenes) structures. Saturated hydrocarbons are non-polar compounds, so the retention of pure, saturated hydrocarbon components is primarily a consequence of the physical size of the gas molecules, i.e., hydrocarbon chain length and degree of branching.

2.4.3. Shale composition

The composition of the reservoir rock is another critical factor that influences the degree of hydrocarbon retention in shale reservoirs. The organic micro-pore volume, gas storage capacity, and the fraction of adsorbed gas in gas-shales have been shown to correlate with TOC (Crosdale et al., 1998; Ross and Bustin, 2009; Zhang et al., 2012). In other words, an organic-rich rock will be able to retain more hydrocarbons than an organic-lean rock. The amount of clay minerals in a source-shale also has an effect on the retention capacity of the shale, as clay minerals can provide additional micro-porosity for gas-storage (Ross and Bustin, 2009; Sondergeld et al., 2010). For this research, the effect of clay minerals on hydrocarbon retention was eliminated by utilizing a shale sample containing almost no clay.

Chapter 3: Adsorption Theory

3.1. Fluid/solid interactions

As stated in the previous chapter, one mechanism by which hydrocarbons are stored and retained in shales is by adsorption on shale kerogen and/or the inorganic mineral matrix. In order to quantify the adsorption processes influencing hydrocarbon retention in organic-rich shales, it is necessary to understand how fluids and solid surfaces can interact with each other. Adsorption is a surface phenomenon marked by an increase in the concentration of a fluid when proximal to a solid surface, due to chemical (chemisorption) and/or physical (physisorption) interactions between the fluid molecules and the surface (Langmuir, 1940; Rouquerol et al., 1999; Barone et al., 2008; Zhang et al., 2012). Chemisorption is a result of site-specific chemical interactions between an adsorbate molecule and an adsorbent surface, in which an adsorbate molecule chemically bonds to and alters the surface of an adsorbent surface. Physisorption occurs due non-specific dispersive interactions between atoms or molecules which do not alter the adsorbent surface; these dispersive interactions are primarily due to van der Waals forces. Sub-section 3.1.1 discusses the differences between specific and non-specific interactions, as well as what kinds of adsorbate molecules and adsorbent surfaces have the ability to interact specifically.

3.1.1. Specific versus non-specific interactions

Specific interactions are intra-molecular interactions that occur due to the concentration of negative or positive charges on the periphery of the bonds and links of interacting systems; non-specific interactions are mainly a result of dipole-induced and/or non-electrostatic inter-molecular/macromolecular forces (Adamson, 1982). Non-specific

interactions exist for all adsorbate/adsorbent systems. The ability of an adsorbate/adsorbent system to interact specifically is dependent on the chemical structure of both the adsorbate molecule and the adsorbent surface (Kiselev, 1965; Bissada, 1968).

Kiselev (1965) proposed a classification scheme for adsorbate molecules and adsorbent surfaces based on their ability to exhibit specific or non-specific molecular interactions. Based on this classification and additions by Bissada (1968), adsorbate molecules may be subdivided into the following four types:

(a) Molecules capable only of non-specific interactions. These possess spherically symmetrical electron shells (inert gases) or only σ-bonds (saturated hydrocarbons).

(b) Molecules capable of specific interactions due to local concentrations of electron density on the peripheries of bonds and links. Examples are given by molecules containing π-bonds (nitrogen gas, unsaturated and aromatic hydrocarbons) and/or atoms with lone electron pairs (oxygen atoms in ethers, ketones, etc.; or nitrogen atoms in tertiary amines, pyridine, etc.).

(c) Molecules capable of specific interactions due to the presence of positive charges on the peripheries of links; molecules containing an active hydrogen atom but no donor atoms are included in this group. Examples include compounds containing 2 or 3 halogen atoms on the same carbon that bears the hydrogen atom ($CHCl_3$, CH_2C1_2, etc.).

(d) Molecules capable of specific interactions due to their possession of functional groups with localized concentrations of electron density and positive charges on the peripheries of links; these molecules are capable of specific interactions with the solid as well as with each other to form mutual hydrogen bonds. For example, molecules of water and alcohols (but not ethers) or ammonia, primary and secondary (but not tertiary) amines possess both lone electron pairs on the oxygen or nitrogen atoms and acidic hydrogens.

The saturated hydrocarbons used as adsorbates in this research are classified as type (a) molecules, and cannot interact specifically. Due to this, interaction energies for the interaction of these molecules with shale or kerogen surfaces should be relatively minor. Molecules of type (b), (c), and (d) were not considered in this research, and so will not be discussed further.

Adsorbents may also be classified based on the electron structure of the atoms and bonds that make up their surface, and are categorized as follows:

I. Adsorbents that have no ions nor active groups. All adsorbate molecules interact with these surfaces non-specifically, with dispersion forces being the main forces of attraction. Examples of such adsorbents include graphitized carbon blacks, and saturated polymers such as Teflon.

II. Adsorbents which have local centers of negative charge on their surface, e.g., π-bonds, or atoms with lone electron pairs as in the case of the oxygen surfaces on

layer silicates, or small-radius anions compensating large complex cations. Such adsorbents are specific for adsorbate molecules of type (c) and (d).

III. The third type includes specific adsorbents containing positively charged small-radius atoms on the surface. Examples may be given by: (i) hydrogen atoms of hydroxyl groups on silica gel and on kaolinite type aluminosilicates, (ii) small-radius cations in large complex anions as in barium sulphate, the zeolites, and the expanding-lattice clay minerals. Such surfaces adsorb specifically molecules of types (b) and (d) (see above).

Both non-specific and specific interaction forces can contribute to the total interaction energy of an adsorbate/adsorbent system, depending on the capacity for adsorbate molecules and the adsorbent surface to exhibit specific interactions. For adsorbate/adsorbent systems that lack the ability for specific interaction, non-specific forces dominate. These non-specific interactions are termed van der Waals interactions, and are discussed briefly in the following sub-section.

3.1.2. van der Waals interactions

Van der Waals interactions are defined as the attractive or repulsive forces between molecules or macromolecules (such as kerogen), other than those resulting from bond formation or the electrostatic interaction of ions or ion groups with each other or neutral molecules (Muller, 1994). These forces include (1) Keesom or orientation forces, which are due to the interaction between two permanent dipoles; (2) Debye or induction forces, which are due to the interaction between a permanent dipole and an induced

dipole; and (3) London or dispersion forces, which are the relatively minor attractive forces that arise between non-polar molecules/macromolecules due to the oscillations in the nuclei-electron systems of each (London, 1930; Dal Nogare and Juvet, 1962; Bissada, 1968; Adamson, 1982). For interactions involving molecules with no dipole moment, such as the saturated hydrocarbons, interaction energies will be a result of dispersion forces only. The magnitude of these dispersion forces varies with the inverse of the distance between the two interacting bodies, and so is primarily dependent on the physical size of adsorbate molecules, and the surface structure/area of the adsorbent (Langmuir, 1940; Adamson, 1982).

3.2. Quantifying hydrocarbon adsorption

The heat of adsorption, ΔH_a, represents the sum of the energy of interactions between adsorbate molecules and an adsorbent surface at low surface coverages, the magnitude of which describes the relative strength by which the adsorbate adsorbs to the surface (Bissada and Johns, 1969; Myers, 2004). Interaction energies can be derived from adsorption isotherms; adsorption isotherms are curves that describe the phase equilibrium between a gaseous adsorbate and a solid adsorbent, at a constant temperature (Dal Nogare and Juvet, 1962; Bissada and Johns, 1969; Myers, 2004). Adsorption isotherms can be determined experimentally via sorption/desorption experiments, and represent the volume of gas that will be adsorbed, per weight of adsorbent, at a particular pressure (see **Figure 3.1**). ΔH_a values for the interaction of hydrocarbons with solid substrates can also be determined via gas-solid chromatography, which was the method used in this research. The chromatographic method and its implications are described in the following section.

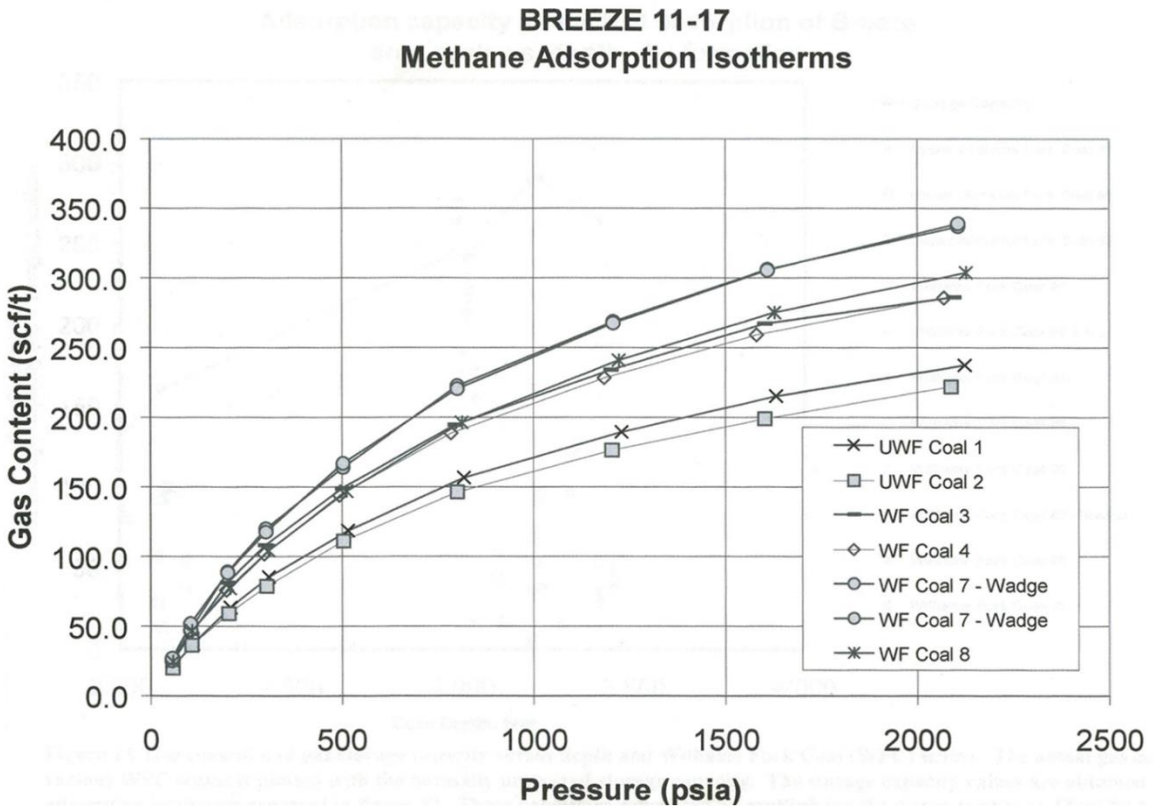

Figure 3.1. Example of adsorption isotherms derived from coal desorption experiments, (Figure from Baker, 2005).

3.3. Gas-Solid chromatography

Previous research has shown that gas-solid chromatography can be used to measure adsorbent-adsorbate interaction energies (Bissada and Johns, 1969; Rybolt et al., 2006; Rybolt et al., 2008). Gas-solid chromatography is a technique by which the components of a mixture are physically separated based on the distribution of such components between a mobile and stationary phase. The mobile phase in gas-chromatography is an inert carrier-gas and the stationary phase is either a solid adsorbent (gas-solid chromatography) or a solid support coated in a liquid stationary phase (gas-

liquid chromatography). **Figure 3.2** shows the basic components of a gas-chromatograph (GC).

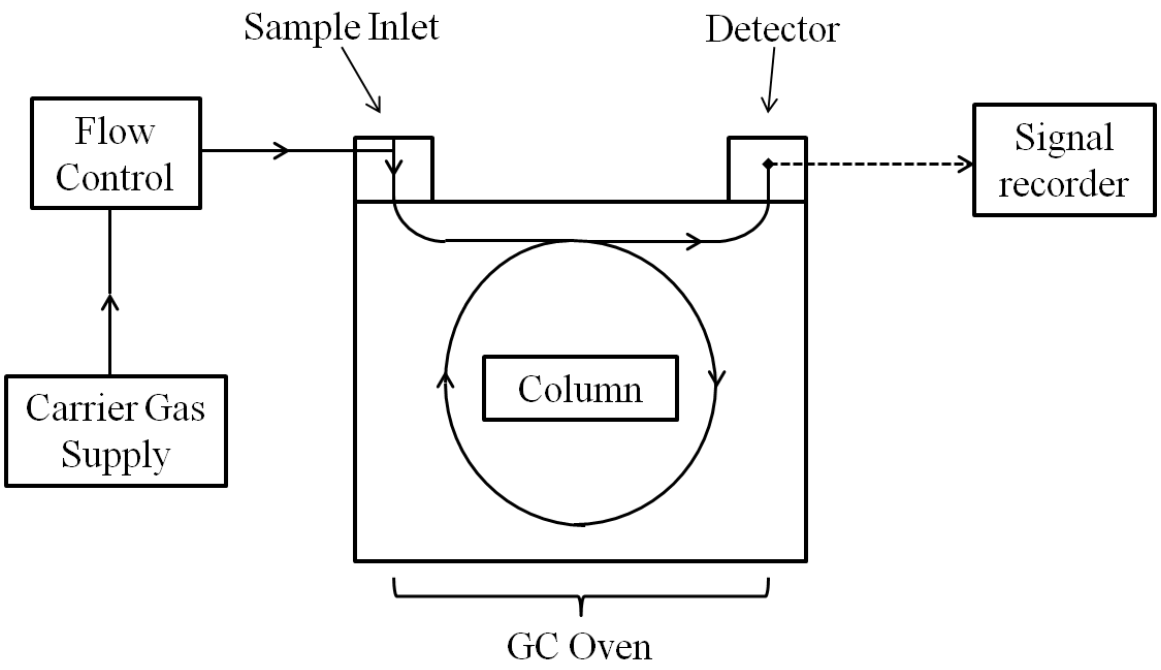

Figure 3.2. Schematic diagram of a gas chromatograph, with direction of flow indicated by arrows.

A column packed with a granular solid adsorbent is installed in the insulated GC oven. Carrier gas, such as helium, continuously flows from a source tank through a flow controller and into the GC. It passes first through the sample inlet, then subsequently flows through the column, past a detector, and finally out of the GC to the atmosphere. When a volatile sample is injected into the carrier gas stream and allowed to pass through the column, the solute vapor is distributed repeatedly in a constant ratio between the carrier gas and the adsorbent. This ratio is determined by the partition coefficient, K,

which is equal to the ratio of the concentration of solute in the adsorbent phase versus the concentration of solute in the gas phase.

Thus, the solute is moved by the carrier gas through the column at a rate which is determined by the solute interaction with the adsorbent. A solute sample will eventually leave the end of the column and enter the detector; the detector response to the eluted solute is recorded as a peak, the magnitude of which is a function of the concentration of sample passing through the detector. The total volume of carrier gas that passes through the column in the time between sample injection and the elution peak maximum (apparent retention time, t'_R) is referred to as the apparent retention volume.

A relation can be made between (1) the apparent retention volume (V'_R) (2) the free gas volume (V_d), (3) the volume of adsorbent (V_a), and (4) the partition coefficient (K), shown as:

$$V'_R = V_d + (K \cdot V_a) \quad (1)$$

where $K = \frac{concentration\ of\ solute\ in\ adsorbent\ phase}{concentration\ of\ solute\ in\ gas\ phase}$

V_d is a theoretically insignificant quantity, since it includes only the total free gas volume between the point of injection and the detector and depends solely on the geometry of the system. As such, a solute's "true" retention volume, V_R, or the volume of carrier gas that flows through the column in the time between the elution of an un-sorbed component (e.g., nitrogen) and the emergence of the solute (true retention time, t_R), can be substituted for $V'_R - V_d$ (see **Figure 3.3**). Thus:

$$V_R = K \cdot V_a \quad (2)$$

This expression implies that the true retention volume of an adsorbate vapor is a function of the partition coefficient and the geometry of the column.

This relationship is valid only if the following assumptions apply:

(i) There is no change in volume of a volume element of carrier gas as it passes through a column. This could result from using low inlet pressures, short columns, and a narrow size range for coarsely ground adsorbent particles.

(ii) The partition coefficient, K, is a constant throughout the column. The concentration of solute on the adsorbent decreases continuously along the column during an elution, so miniscule sample volumes are used to approximate the condition of infinite dilution even at the injection end of the column.

(iii) No adsorbate-adsorbate, adsorbate-carrier gas, or carrier gas-carrier gas interactions exist in the vapor phase above the adsorbent. Small samples of solute eliminate adsorbate-adsorbate interactions, while the use of an inert carrier gas eliminates the possibility of adsorbate-carrier gas or carrier gas-carrier gas interactions.

(iv) The surface available for adsorption must not be a function of the physical state of subdivision of the adsorbent.

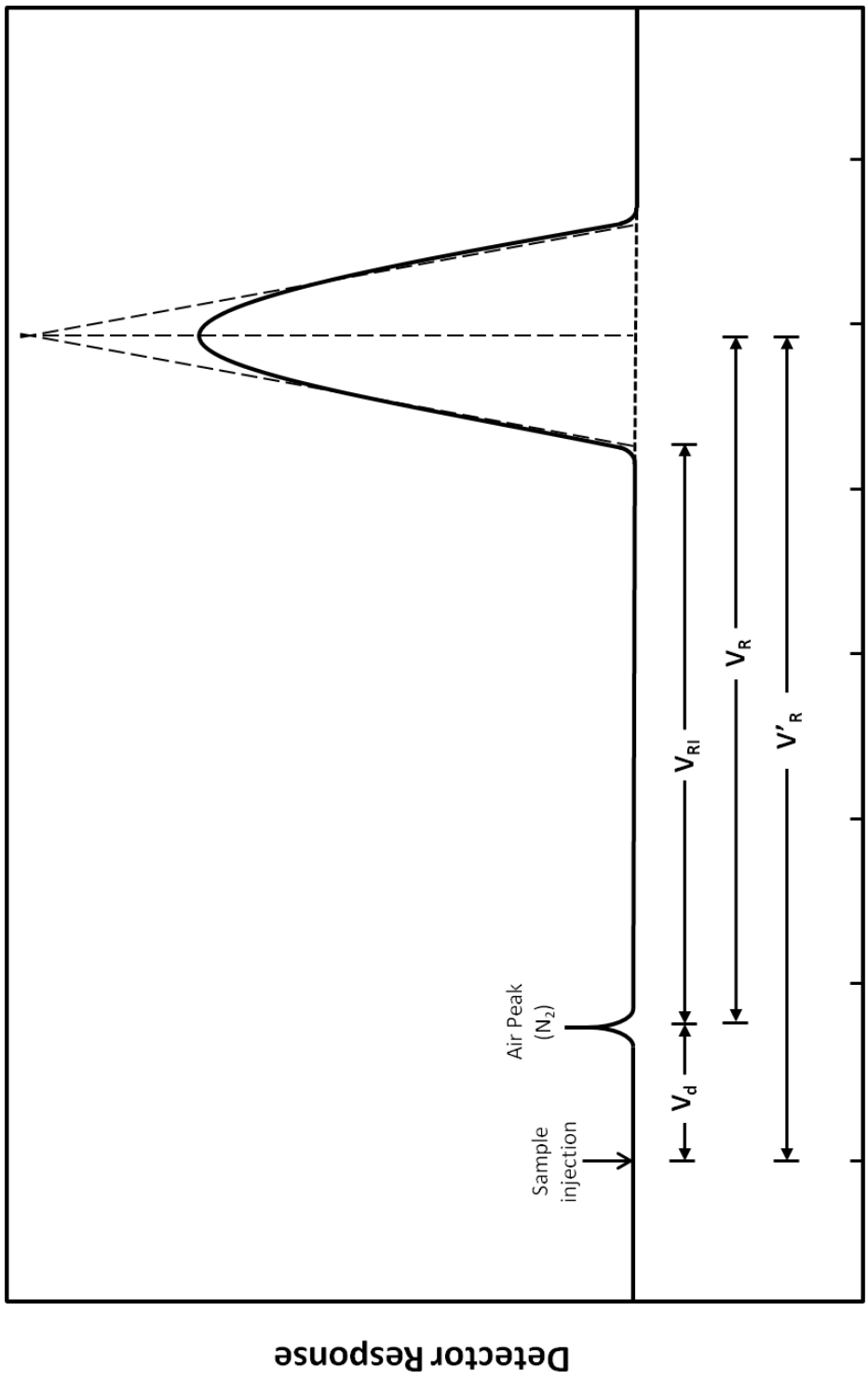

Figure 3.3. Typical gas chromatograph elution curve, (Figure reproduced from Bissada (1968) with permission).

It has been observed that in runs at constant flow rate, but increasing sample size, the location of the peak maximum varies; i.e., the peak retention volume, and consequently the true retention time, depends on sample size (Dal Nogare and Juvet, 1962; Bissada, 1968). The peak width must approach zero in the limiting conditions of zero sample size (infinite dilution), which suggests that the initial retention time (t_{RI}) and the corresponding initial retention volume, V_{RI}, are the significant quantities; so:

$$V_{RI} = K \cdot V_a \tag{3}$$

By substituting $\frac{W_a}{\rho_a}$ for V_a in equation (3) and re-arranging the variables, the expression becomes:

$$\frac{V_{RI}}{W_a} \cdot \rho_a = K \tag{4}$$

where V_{RI} = initial true retention volume

W_a = weight of adsorbent

ρ_a = density of adsorbent

K = partition coefficient

For simplification purposes, $\frac{V_{RI}}{W_a}$ is defined as the specific retention volume, V_g, which is qualitatively defined as the volume of gas required to elute one half of the solute from a column containing one gram of stationary phase with no pressure drop or free gas space. So:

$$V_g \cdot \rho_a = K \tag{5}$$

The partition coefficient, K, describes the adsorption equilibrium and is temperature dependent; this temperature dependence is described by the exponential relation:

$$K = C \cdot e^{-\Delta H_a/RT} \tag{6}$$

in which C is a constant, ΔH_a is the heat of adsorption, T is the absolute temperature, and R is the molar gas constant. It is an exothermic process, and K decreases with increasing T.

Taking the natural logarithm of the equation yields:

$$\ln K = -\Delta H_a/RT + \ln C \tag{7}$$

Equation 5 defined the partition coefficient K in terms of V_g, such that:

$$ln(V_g \cdot \rho_a) = -\Delta H_a/RT + \ln C$$

and

$$\ln V_g = -\Delta H_a/RT + \ln C - \ln \rho_a \tag{8}$$

Over relatively small temperature intervals, variations in the solid phase density with temperature are negligible and are assumed constant; as such, ln ρ_a and ln C may be substituted by a constant C_1 in equation (8), so that:

$$\log_{10} V_g = -\Delta H_a/2.303\ RT + C_1 \tag{9}$$

Differentiation this equation with respect to 1/T gives the following:

$$\frac{d \log_{10} V_g}{d\frac{1}{T}} = -\Delta H_a/2.303\ R \tag{10}$$

When the equation is arranged to solve for the heat of adsorption it becomes:

$$\Delta H_a = -2.303\ R\ \frac{d(\log_{10} V_g)}{d(1/T)} \quad (11)$$

By this relation, the heat of interaction, ΔH_a, of a solid stationary phase with a solute vapor carried in an inert mobile gas phase is related to the chromatographic 'specific retention volume', V_g. Thus, a plot of $\log_{10} V_g$ versus 1/T will have a slope of $-\Delta H_a/2.303R$. If R is given as 1.987×10^{-3} kcal/mol deg., ΔH_a will have units of kcal/mol.

Dal Nogare and Juvet (1962) discuss the limitations of gas-solid elution analysis, which include (a) irreversible adsorption, (b) variable activity of adsorbents, (c) catalytic effects on adsorbent surfaces, and (d) excessive retention of polar molecules. Factors (a) and (b) are related, and a column that is repeatedly used will lose activity; factor (b) is also observed when a column is used over an extended temperature range. Factor (c) is seen for compounds that can undergo polymerization or rearrangement on active surfaces, resulting in variable retention times or irreversible loss of the compound. Factor (d) restricts the gas-solid elution technique to relatively inert gases and vapors. These effects were avoided in this research by using relatively inert adsorbates (saturated hydrocarbons) and adsorbents with limited surface activity (clay-poor shale/immature kerogen).

The gas-chromatographic approach has been successfully used to measure ΔH_a values for the interaction of saturated hydrocarbons with graphitized carbon black, carbon powders, and zeolites (Ross et al., 1962; Ligner et al., 1990; Rybolt et al., 2006; Rybolt et

al., 2008). Prior to this research, the chromatographic method has not been used to measure ΔH_a for the interaction of light hydrocarbons with kerogen.

Chapter 4: Methods

4.1. Samples and initial preparation

The samples examined in this study include a whole-rock Green River shale, and a kerogen isolated from the same shale. The whole-rock was sampled from the Mahogany Ledge zone of the Parachute Creek member of the Green River Shale Formation, which is located in the Piceance Basin of northwestern Colorado (**Figure 4.1**). The Mahogany Ledge zone of the Green River shale is thermally immature and is composed of Eocene-age sediments which were originally deposited in a shallow-lacustrine environment (Robinson, 1969; Ibrahimov and Bissada, 2010). The Mahogany zone is particularly organic-rich, and differs compositionally from the traditional definition of a shale (clay-rich, primarily siliciclastic rocks); the Mahogany Ledge "shale" is technically an organic-rich calcareous marlstone (clay-poor, carbonate) (Robinson, 1969; Speight, 2013). The Green River Shale Formation contains several members containing variable amounts of organic matter and clay minerals; the Mahogany zone was sampled specifically for this research because of its organic-richness and low clay content.

Initial sample preparation began with the Green River shale sample being ground in a SPEX Shatterbox and then sieved to retain the 40-60 mesh (250-400 microns) fraction for adsorption experiments. An aliquot of the ground shale was powdered for geochemical characterization. Kerogen was chemically-isolated from the whole-rock shale via the method described by Ibrahimov and Bissada (2010). The isolated kerogen was powdered with a mortar and pestle for adsorption experiments and geochemical characterization. The ground and powdered samples were degassed in a vacuum oven overnight at 80^{o}C to remove any adsorbed water.

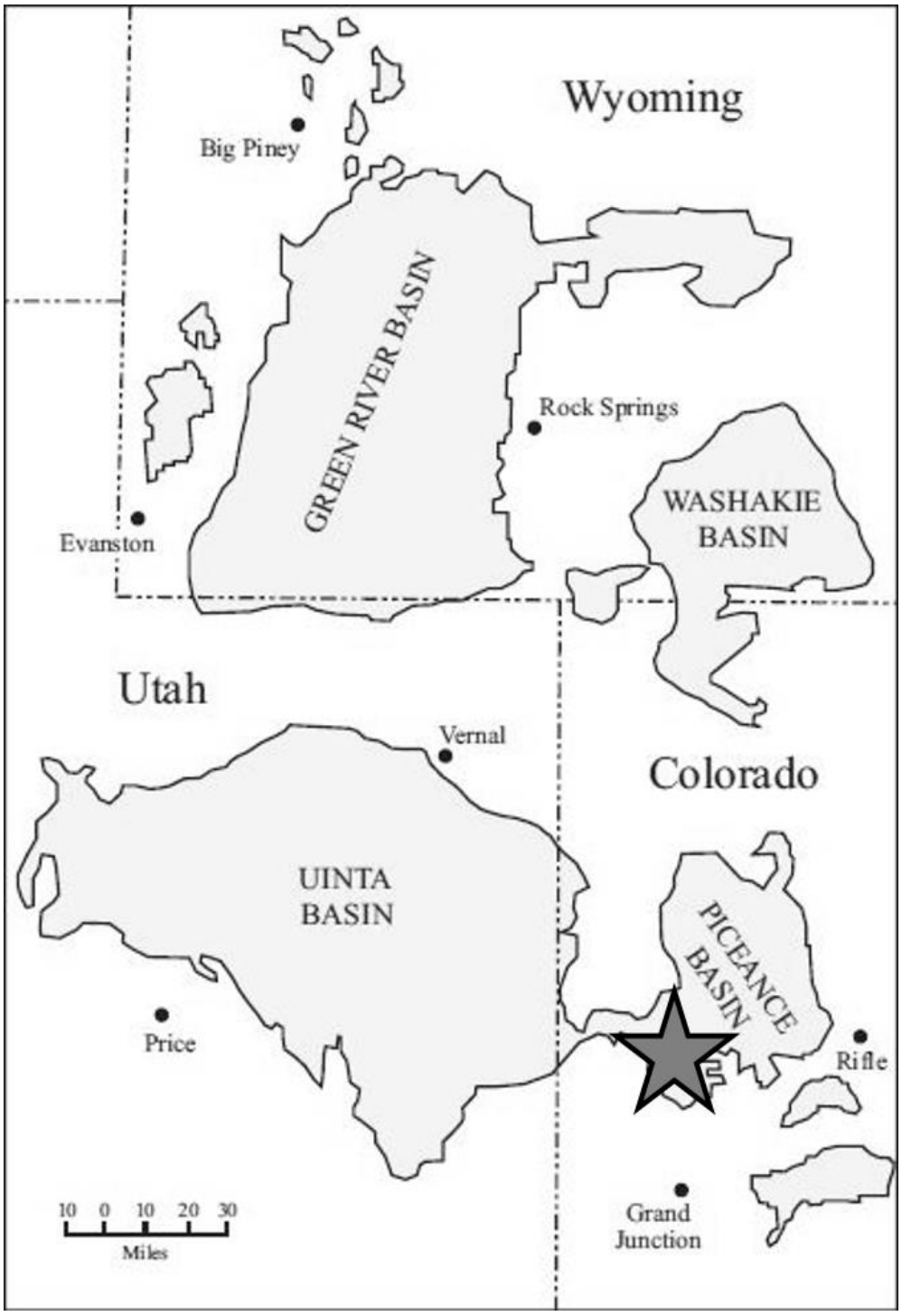

Figure 4.1. Map of basins containing the Green River Formation, with the approximate sample collection location in the Piceance basin marked with a star, (figured adapted from Vanden Berg, 2008).

Bitumen was solvent extracted from the vacuum-dried kerogen and shale aliquots prior to their use in adsorption experiments. The solvent-wet samples were allowed to air-dry, and were then placed in a vacuum oven overnight at 80°C to remove any residual solvent.

4.2. Sample characterization

4.2.1. Total organic carbon

Total organic carbon (TOC) analysis was done on aliquots of the native and solvent-extracted shale. TOC is a measure of the organic richness of a sample, and is a general indicator of petroleum generation potential. Prior to instrumental analysis, a small amount of powdered shale was placed in a porous ceramic crucible. The sample was acidized overnight with concentrated hydrochloric acid (HCl) to remove inorganic carbonate minerals, such as calcite and dolomite. After acid treatment, the sample was washed with water and dried overnight in an oven. Once dry, the sample was run through a LECO Carbon/Sulfur Combustion Analyzer to determine TOC. The instrument works by combusting samples with ultra-high purity oxygen to form CO_2, which is analyzed for carbon content using an infrared detector. Carbon values are reported in weight percent (wt %).

4.2.2. X-ray diffraction

X-ray powder diffraction (XRD) was conducted on the solvent extracted shale to determine the general mineralogy; XRD was also done on the isolated kerogen to identify inorganic contaminants remaining post-isolation. XRD is a non-destructive analysis in which a sample is placed between an x-ray source and an x-ray detector at different

orientations; the sample is bombarded with focused x-rays of a known wavelength, and the diffraction pattern of the reflected radiation is recorded. Minerals have unique crystal lattice structures defined by the arrangement of atoms in parallel planes, and reflect x-ray radiation at different intensities based on the spacing between the lattice planes ("d"-spacing) (Dinnebier and Billinge, 2008). The relative intensity of reflected x-rays is plotted against the diffraction angle (θ), and the resulting pattern can be interpreted for mineral identification. For this study, XRD measurements were made using a Siemens D5000 diffractometer equipped with a copper K-alpha radiation source. A powdered sample of shale or kerogen was placed on a zero-background holder and loaded into the diffractometer; standard XRD methods were used and a diffraction pattern was generated. Mineral identification was done by cross-referencing the generated diffraction patterns with a dataset provided by the International Center for Diffraction Data (ICDD).

4.2.3. Kerogen ash-content

Ash-content analysis was conducted on the Green River kerogen to assess kerogen purity. Ash content was measured by placing a small amount of sample in a ceramic crucible, and combusting the sample in a furnace overnight at ~800°C. The weight of the crucible pre- and post-combustion was determined, with the difference representing the total ash content of the sample. The ash indicates the amount of inorganic minerals left in the kerogen, post-isolation. Ash content was reported as a percentage of the total sample weight (wt %).

4.2.4. Organic elemental analysis

Organic elemental analysis was done on the isolated kerogen to confirm the kerogen type, and to assess the thermal evolution of the organic matter. Elemental analysis results were plotted as H/C and O/C atomic ratios on a van Krevelen diagram. A Perkin Elmer 2400 CHN Analyzer fitted with an oxygen accessory kit was used to determine kerogen elemental composition in wt % of carbon, hydrogen, nitrogen, and oxygen. The instrument works by combusting samples with ultra-high-purity oxygen to form carbon dioxide (CO_2), water vapor (H_2O), and/or nitrogen gas (N_2); the generated gases were separated using chromatography and quantified with a thermal conductivity detector (TCD). The instrument determines oxygen content via pyrolysis, which converts oxygen in the sample to carbon monoxide (CO); the CO was separated from other pyrolysis products via chromatography and quantified with a TCD.

4.3 Hydrocarbon adsorption measurements

4.3.1. Gas-solid chromatography

Following geochemical characterization, 2.976 grams of the degassed kerogen and 11.705 grams of the degassed shale were individually packed into two-foot columns fabricated from 1/4" O.D. chromatographic-grade copper tubing. Both ends of each column were sealed with a glass wool plug. Each packed column was installed on a Hewlett-Packard 5890A Series gas-chromatograph (GC) equipped with a TCD operating at 250°C. Elution curves were recorded using HP CORE ChemStation software on a desktop PC. Ultra-high-purity helium was used as carrier gas; the flow rate was determined via a soap-film flow meter, and was held constant at 60 mL/min for all runs.

The outlet pressure was atmospheric. The inlet pressure was measured with a pressure gauge, and was adjusted based on the studied substrate and column temperature. Column temperatures were measured by the GC oven thermostat, while ambient temperature was determined with a glass thermometer. Samples of hydrocarbon gas were introduced into the carrier gas stream by means of a pneumatically controlled constant-volume sampling loop; nitrogen was used as a tracer gas to simulate an air peak. Injected sample volumes were 250 micro-liters (μL). Column temperature was held constant during runs, and retention times for C2, C3, i-C4, and n-C4 on the kerogen and shale adsorbents were determined at 30, 40, 50, 60, 70 and 80°C. Retention time measurements for methane were attempted at 30, 35, 40, 45 and 50°C but were unsuccessful due to lack of retention at all temperatures, for both the kerogen and the shale adsorbents. Before making a series of runs, the column oven temperature was adjusted to 90°C, the detector-end of the column was detached, and the packed column was allowed to condition overnight under a constant helium flow. Following conditioning, the column was re-attached to the detector, the oven temperature was adjusted to the highest planned run temperature, and the system was allowed to equilibrate thermally for 2 hours. The detector response was monitored after re-attaching the column to ensure that no hydrocarbons were generated from the kerogen due to the column conditioning. Following thermal equilibration, a series of helium blanks were injected to confirm there were no residual hydrocarbons remaining in the column, the column flow-rate was determined, ambient temperature and pressure were recorded, a gas sample was injected, and an elution curve was generated.

4.3.2. Heat of adsorption determination

After the initial chromatographic retention times for each hydrocarbon gas were measured on the shale and kerogen substrates, the specific retention volume (V_g) was calculated by the relation established in Equations 4 and 5, and by Bissada and Johns (1969), as follows:

$$V_g = \frac{V_{RI}}{W_a} = \frac{t_{RI} \cdot F_c \cdot j}{W_a} \quad (12)$$

where V_{RI} = initial retention volume

t_{RI} = initial retention time

F_c = flow rate of carrier gas in mL/min, corrected to column temperature, T_c, and outlet or ambient pressure, P_a; thus:

$$F_c = F \cdot \left(\frac{T_c}{T_a}\right) \cdot \left(1 - \frac{P_w}{P_a}\right) \quad (13)$$

F = measured flow rate at ambient temperature, T_a
P_w = vapor pressure of water at T_c; since a soap-film meter was used, this is needed to correct for vapor pressure of water. Values were derived from Haar et al. (1984).

j = compressibility factor for the gas, in terms of the inlet pressure, P_i, and outlet pressure, P_o, as:

$$\frac{3\left[(P_i/P_o)^2 - 1\right]}{2\left[(P_i/P_o)^3 - 1\right]}$$

W_a = weight of adsorbent used as column packing.

Initial retention times (t_{RI}) were all <1 minute, and varied depending on column temperature and the studied adsorbent. After each run, the system was allowed to flush itself of residual hydrocarbons under helium-flow for at least one hour. After a set of runs

was completed for an isotherm, the GC oven temperature was adjusted to the next lower temperature value, and the system was allowed to thermally equilibrate for at least 2 hours. Following thermal equilibration, the flow rate was determined, and the next sample was injected.

The standard deviation of the measured retention times and V_g values was determined for the retention of ethane and propane in the kerogen and whole-rock adsorbent columns. The precision of the retention measurements for i-butane and n-butane on the kerogen could not be determined due to the limited amount of runs conducted at each temperature. A plot of $\log_{10}V_g$ vs. 1/T was made for each hydrocarbon gas off of the shale and kerogen substrates, demonstrated by **Figure 4.2**. The heat of adsorption (ΔH_a) was calculated for each hydrocarbon gas off of each shale and kerogen substrate, based on the relationship of the slope of the line to ΔH_a, shown by **Equation (1)** (Bissada and Johns, 1969). The standard deviation of ΔH_a values for the interaction of ethane and propane with the kerogen and whole-rock shale was determined from the slopes of the plots of $\log_{10}V_g$ vs. 1/T for the minimum and maximum calculated V_g values; the standard deviation of ΔH_a values calculated for i-butane and n-butane could not be determined due to the limited retention data.

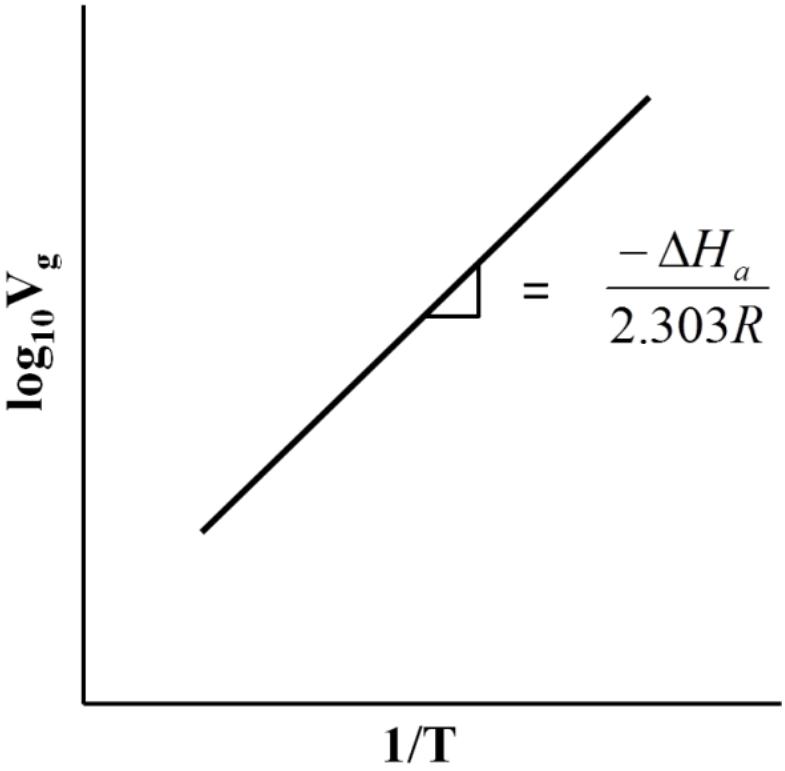

Figure 4.2. Correlation plot of specific retention volume (V_g) as a function of temperature (T). Heats of adsorption can be determined from the slope of the plotted line, (Bissada and Johns, 1969).

Chapter 5: Results and Interpretation

5.1. Sample characterization

The native Green River shale has a TOC content of 13.15%, while the solvent-extracted shale, used as an adsorbent in this study, has a TOC content of 11.95%; these values reflect the organic richness of the shale. The drop in TOC values for the extracted rock versus the whole-rock is due to the relatively high bitumen content.

X-ray diffraction confirms that the studied Green River shale is a dolomitic, clay-poor rock, with some silicate minerals, (**Figure 5.1**). The lack of surface active clay minerals suggests that the inorganic shale minerals lack the capacity for specific interaction.

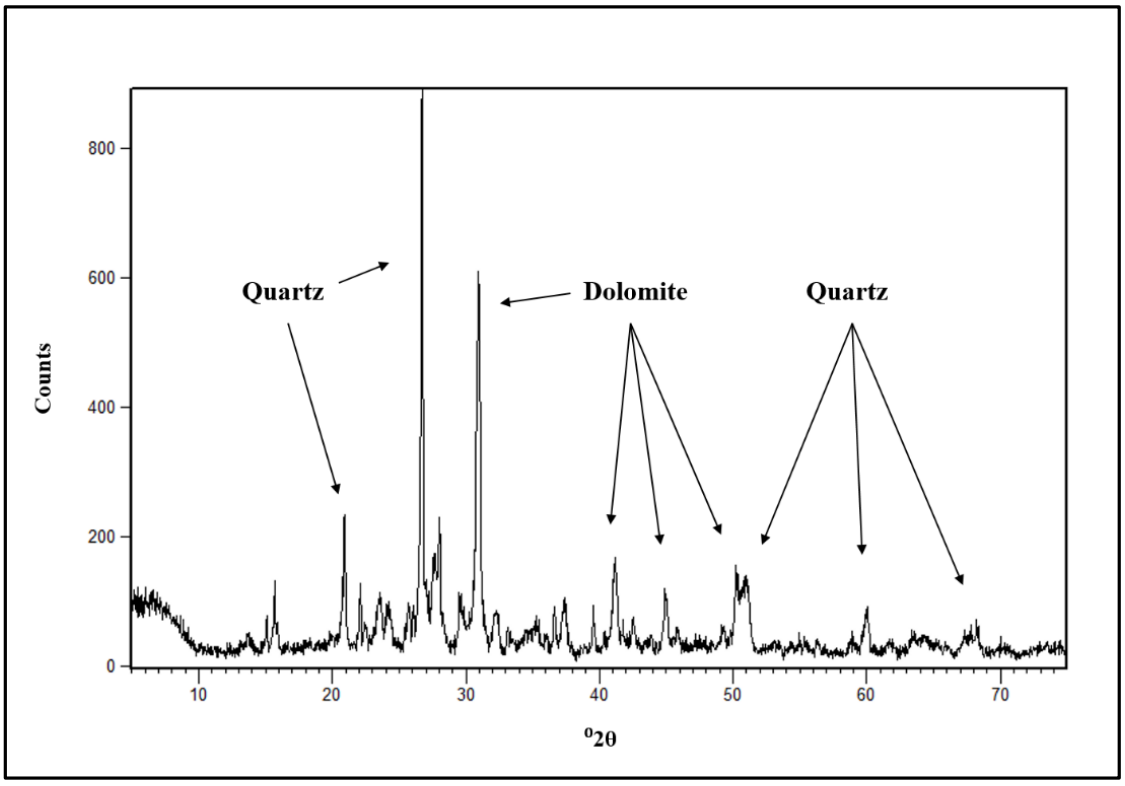

Figure 5.1. X-ray diffractogram of the solvent-extracted Green River shale, with major mineral components identified.

Elemental analysis of the solvent-extracted Green River kerogen shows that the kerogen is composed of 70.02% C, 8.92% hydrogen, 2.11% nitrogen, and 7.42% oxygen, by weight. The kerogen hydrogen/carbon (H/C) and oxygen/carbon (O/C) ratios were determined to be 1.52 and 0.08, respectively. When plotted against each other on a modified van Krevelen diagram, the H/C and O/C atomic ratios confirm that the kerogen is a Type I immature kerogen (**Figure 5.2**). Ash-content and x-ray diffraction (XRD) analysis show the isolated kerogen residue to be 94.3% pure kerogen, with 5.7% pyrite residue (**Figure 5.3**).

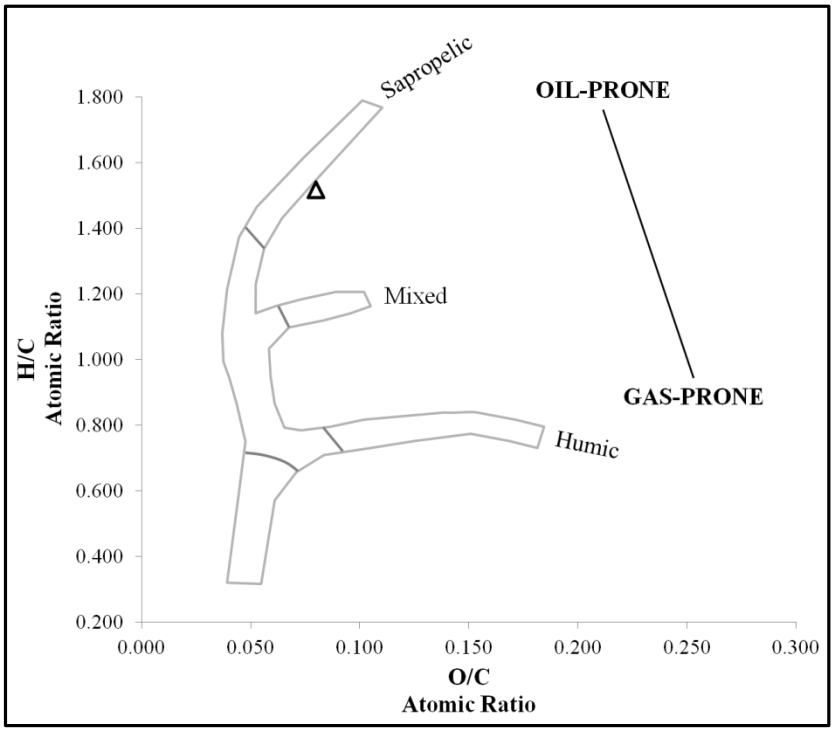

Figure 5.2. Modified van Krevelen diagram plotting measured H/C vs O/C atomic ratios for the Green River kerogen

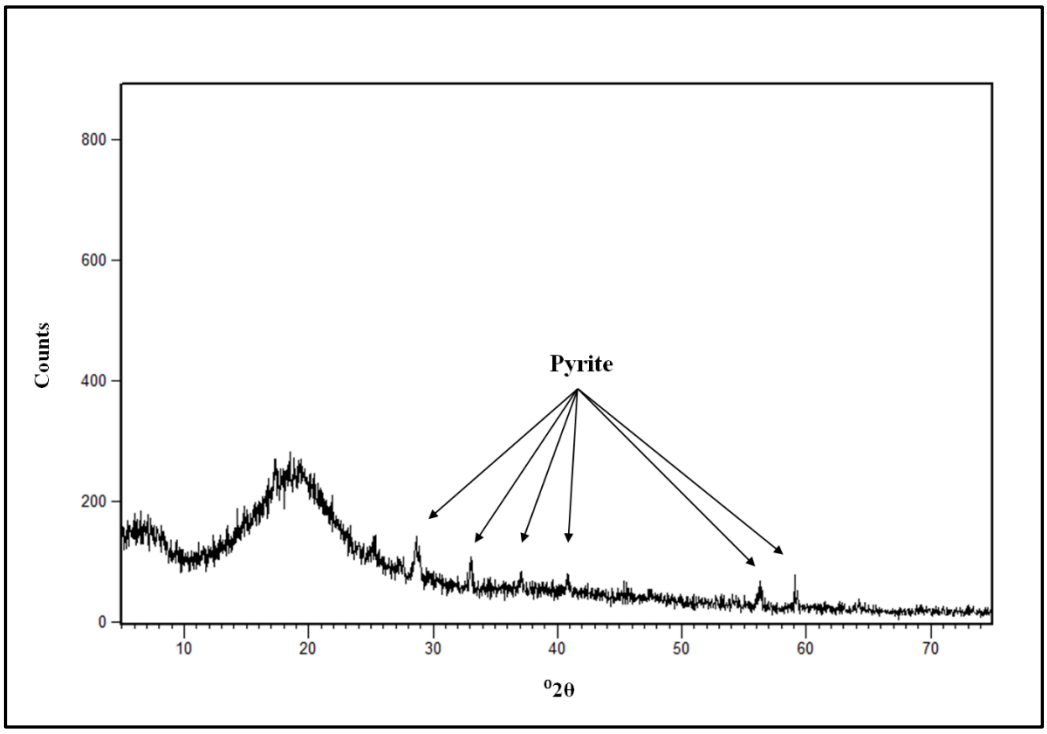

Figure 5.3. X-ray diffractogram of the isolated Green River shale kerogen, with major inorganic components identified.

5.2. Hydrocarbon adsorption measurements

5.2.1. Hydrocarbon retention

The average experimental retention data for the adsorption of the light hydrocarbon components on the Green River kerogen and whole shale are presented in **Table 2** and **Table 3**. Calculated standard deviations for the measured retention times and V_g values are minimal, which proves the measurements to be precise. The temperature dependence of adsorption is reflected by larger retention times measured at lower temperatures. Retention times for C2-C3 on the kerogen adsorbent are very small and are between 0.1 – 0.8 min; retention times for the same gases on the shale adsorbent are much smaller, and are between 0.03 - 0.05 minutes. Retention times for C2-C3 increase

with carbon number for adsorption on both the kerogen and whole-rock adsorbents; V_g values are less linear, but display the same trend of increasing with carbon number and decreasing with increasing temperature. The Green River kerogen adsorbent has longer retention times and larger V_g values for C2-C3 at all temperatures, compared to the whole-rock shale.

Table 2. Average experimental retention data and calculated standard deviation for the retention of ethane, propane, i-butane, and n-butane on the kerogen.

Retention on the Kerogen

Adsorbate	Column temp. (^{0}C)	T_{RI} (min)	T_{RI} Std. Dev. (min)	V_g (mL)	V_g Std. Dev. (mL)
Ethane (C2)	30	0.126	+/- 0.000	1.389	+/- 0.005
	40	0.113	+/- 0.000	1.257	+/- 0.004
	50	0.106	+/- 0.000	1.153	+/- 0.003
	60	0.102	+/- 0.001	1.081	+/- 0.004
	70	0.095	+/- 0.000	1.007	+/- 0.003
	80	0.085	+/- 0.000	0.899	+/- 0.004
Propane (C3)	30	0.243	+/- 0.001	1.389	+/- 0.008
	40	0.225	+/- 0.000	1.257	+/- 0.004
	50	0.205	+/- 0.000	1.153	+/- 0.003
	60	0.187	+/- 0.001	1.081	+/- 0.012
	70	0.167	+/- 0.000	1.007	+/- 0.002
	80	0.148	+/- 0.004	0.899	+/- 0.021
i-Butane (i-C4)	30	0.169		1.803	
	40	0.181		1.914	
	50	0.188		1.970	
	60	0.191		1.975	
	70	0.183		1.883	
	80	0.172		1.792	
n-Butane (n-C4)	30	0.810		8.662	
	40	0.675		7.156	
	50	0.557		5.893	
	60	0.463		4.778	
	70	0.370		3.885	
	80	0.325		3.348	

Retention times for the adsorption of i-C4 on the kerogen are between 0.17 - 0.19 min; n-C4 has retention times between 0.6 – 1.1 min. i-C4 has shorter retention times and smaller V_g values on the kerogen adsorbent than both C3 and n-C4. Retention data for the adsorption of i-C4 does not increase linearly with temperature, and anomalous values were removed for adsorption energy calculations so a linear relationship could be established. N-C4 has the greatest range of retention time and V_g values on the kerogen adsorbent versus temperature, than do all other studied gases.

Table 3. Average experimental retention data and calculated standard deviation for the retention of ethane and propane on the whole-rock.

Retention on the Whole-Rock

Adsorbate	Column temp. (^{0}C)	T_{RI} (min)	T_{RI} Std. Dev. (min)	V_g (mL)	V_g Std. Dev. (mL)
Ethane (C2)	30	0.028	+/- 0.000	0.117	+/- 0.001
	40	0.025	+/- 0.000	0.104	+/- 0.001
	50	0.023	+/- 0.000	0.100	+/- 0.001
	60	0.020	+/- 0.000	0.089	+/- 0.001
	70	0.019	+/- 0.000	0.087	+/- 0.001
	80	0.018	+/- 0.000	0.084	+/- 0.001
Propane (C3)	30	0.049	+/- 0.000	0.202	+/- 0.001
	40	0.042	+/- 0.000	0.179	+/- 0.000
	50	0.036	+/- 0.000	0.158	+/- 0.000
	60	0.032	+/- 0.000	0.143	+/- 0.001
	70	0.028	+/- 0.000	0.127	+/- 0.002
	80	0.025	+/- 0.001	0.118	+/- 0.003

5.2.2. Hydrocarbon heats of adsorption

The heat of adsorption for the interaction of each gas with the kerogen and shale adsorbents was determined from the slope of the plot of $\log_{10}V_g$ vs. 1/T (**Figure 5.4**). For i-C4, retention volumes determined at 30, 40, and 50°C were not used in the calculation

of ΔH_a due to inconsistencies in the data. The interaction energies for C2, C3, i-C4, and n-C4 with the Green River kerogen, and C2 and C3 with the parent shale are presented in **Table 4**. The standard deviation of ΔH_a values calculated for the interaction of ethane with both adsorbents is no greater than 0.03 kcal/mol; the standard deviation of ΔH_a values calculated for the interaction of propane with both adsorbents is no greater than 0.07 kcal/mol. The standard deviation data show that the variation between the average and minimum/maximum ΔH_a values is minimal. ΔH_a values for C2, C3, n-C4, and i-C4 off of the kerogen adsorbent were measured to be -1.76, -2.23, -4.13, and -1.14 kcal/mol, respectively. ΔH_a values for the interaction of C2 and C3 with the whole shale were determined to be -1.40 kcal/mol and -2.32 kcal/mol, respectively. ΔH_a values increase with hydrocarbon molecule carbon number for interactions with both the shale and kerogen adsorbents. Adsorption energies for the interaction of C2 and C3 with the Green River kerogen were similar to those determined for interaction of the same gases with the whole-rock shale. ΔH_a values for the interaction of i-C4 with the kerogen are less than ΔH_a values for the interaction of C2, C3, and n-C4 with the same adsorbent.

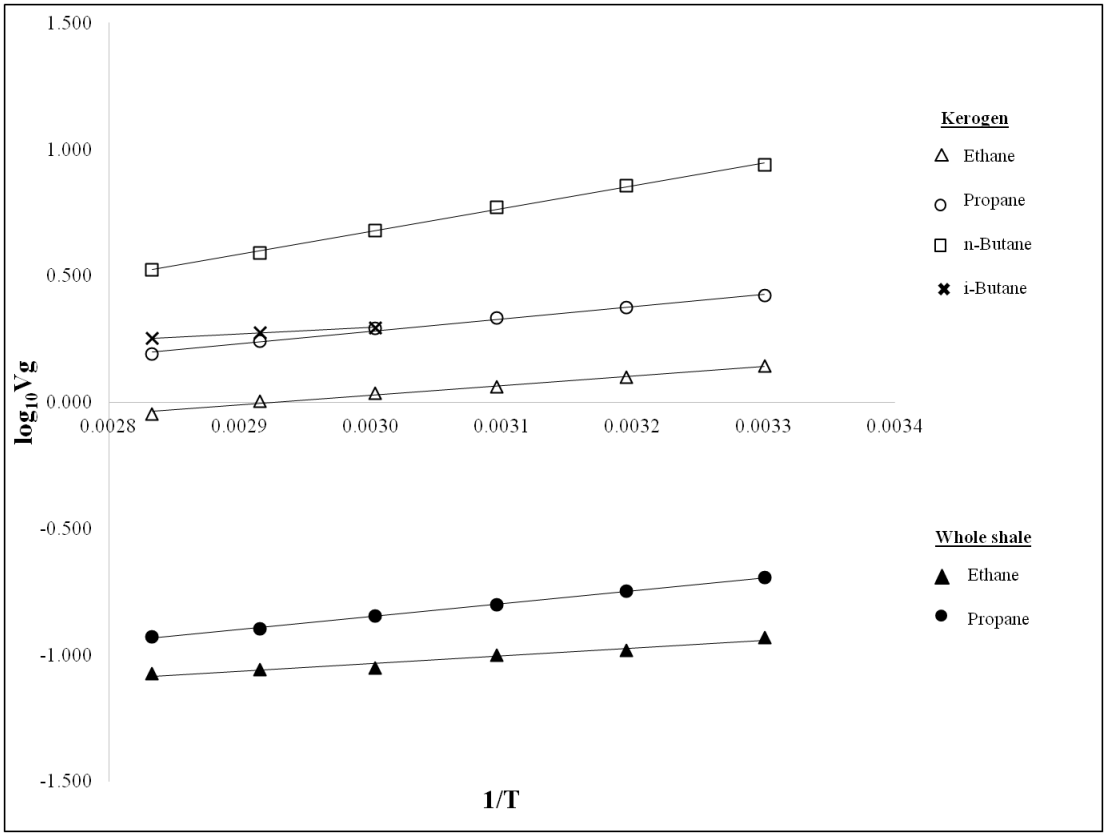

Figure 5.4. Variation of $\log_{10}$Vg versus 1/T for hydrocarbon adsorption on the Green River kerogen and whole rock shale.

Table 4. Measured heats of adsorption and standard deviation for the interaction of C2-C3 and i-C4 with the Green River kerogen, and C2-C3 with the Green River shale.

Adsorbent	Adsorbate	ΔH_a (kcal/mol)	Std. Deviation (kcal/mol)
Green River kerogen	Ethane	- 1.76	+/- 0.00
	Propane	- 2.23	+/- 0.03
	n-Butane	- 4.13	
	i-Butane	- 1.14	
Green River shale	Ethane	- 1.40	+/- 0.03
	Propane	- 2.32	+/- 0.07

Chapter 6: Discussion

6.1. Specificity of measured interaction energies

All ΔH_a values determined in the current study are too low to be considered a result of chemical adsorption; interaction energies of less than ~10-12 kcal/mol can be assumed to be a result of non-specific dispersion forces (Adamson, 1982; Xia and Tang, 2012). Based on this definition, and the inability of saturated hydrocarbons to interact specifically, it is concluded that the measured interaction energies for all gases on both adsorbents are due to non-site-specific interactions only. It is projected that larger ΔH_a values would be observed for fluid/solid interactions involving heavier n-alkane molecules, and that the volume of retained hydrocarbons would increase as a result.

6.2. Role of the matrix minerals in hydrocarbon adsorption

The similarity between ΔH_a values determined for the kerogen and the whole-rock can be explained as consequence of the whole-rock mineralogy. The Green River shale is primarily composed of carbonate minerals. Carbonate minerals do not have the capacity for significant interactions with organic molecules (Rigo et al., 2012). As such, hydrocarbon/inorganic interactions will be negligible. The similarity between ΔH_a values determined for the interaction of C2 and C3 with kerogen and the whole-rock suggests that the inorganic matrix minerals in the whole-rock shale have almost no impact on the potential of the rock to adsorb hydrocarbons. The lack of surface-active clay minerals in the Green River shale even further limits the potential of the whole-rock for interaction with the hydrocarbon gases. Based on these findings, it is concluded that the kerogen has the dominant role in the retention and adsorption of hydrocarbons, for this system.

6.3. Steric influences on hydrocarbon adsorption

As expected, ΔH_a values increase with molecular mass for the n-alkanes. However, the interaction energy determined for i-butane on the kerogen is less than that determined for n-butane, even though both compounds have the same molecular mass. This difference can be attributed to the greater distance between the center of mass and molecule peripherals for i-C4 versus n-C4, as the relative force of molecular interactions correspond to the inverse of the distance between the mass (or charge) centers of interacting species (Adamson, 1982). The relationship between the force of attraction and the distance between two masses is described by Newton's law of universal gravitation, as follows:

$$F = \frac{G*M1*M2}{r^2} \tag{14}$$

where F = the force between two mass centers

G = the gravitational constant

M1 = first mass

M2 = second mass

r = distance between the two masses

A visual representation of this explanation is presented in **Figure 6.1**. For simplification purposes, and due to the immature and amorphous nature of the Green River kerogen, the kerogen surface is assumed to be homogenous and to have a constant mass (M1). N-C4 and i-C4 have the same molecular mass (M2), so the magnitude of the

force of non-electrostatic interactions between these molecules and the kerogen is controlled by the distance (r) between mass centers of the adsorbent kerogen surface and adsorbate hydrocarbon molecules. The re-arrangement of the methyl group in i-C4 effectively increases the distance between the molecule's center of mass and the kerogen adsorbent surface, relative to n-C4. As a consequence, the energy of interaction for i-C4 with the kerogen adsorbent is less than the energy of interaction for n-C4 with the same adsorbent.

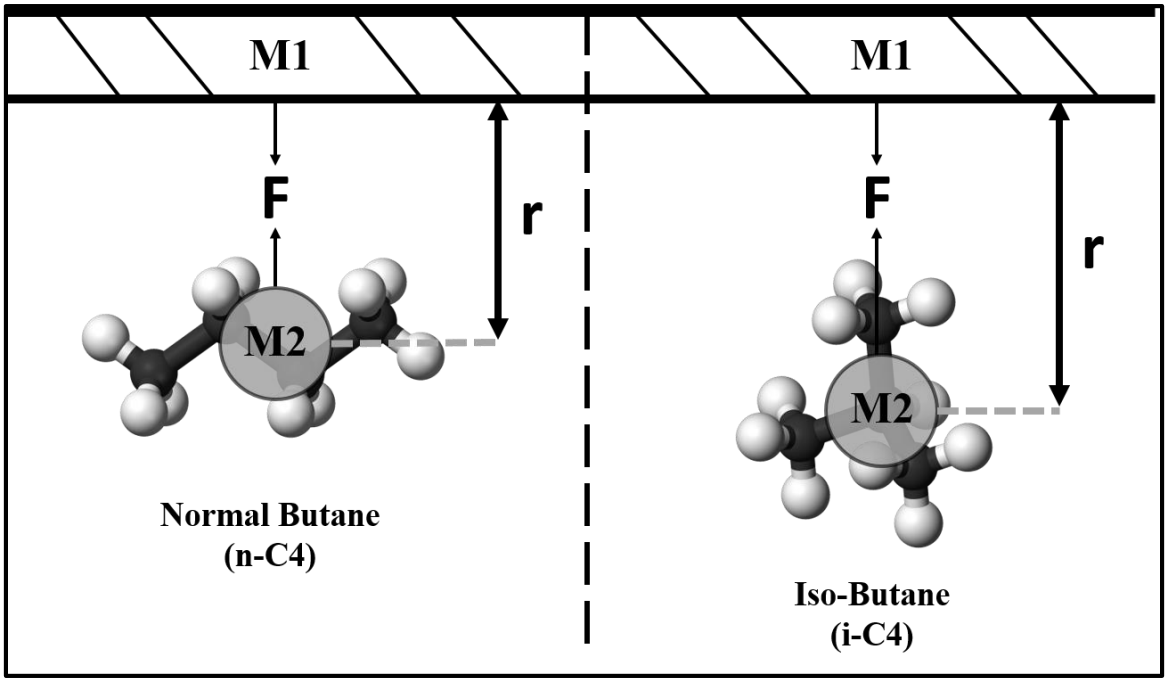

Figure 6.1. Visual representation of the relative magnitude of the force of interaction for i-C4 versus n-C4 with a solid surface, based on Newton's law of universal gravitation.

Based on these results, it is concluded that the physical structure of the adsorbate hydrocarbon molecules has a significant control on the magnitude of the measured interaction energies, and that adsorption energies are not just a function of the adsorbate molecular mass. The relative contribution of an adsorbate's molecular diameter to

intermolecular/macromolecular interactions will decrease for adsorbates/adsorbents with greater electrostatic potentials, but for experiments utilizing adsorbate molecules with no electrostatic potential (such as the saturated hydrocarbons) the influence of the adsorbate molecular diameters is non-negligible.

6.4. Influences on organic/organic interactions

6.4.1. Organic-carbon content of the kerogen versus the whole-rock

The greater hydrocarbon retention times on the kerogen are likely attributed to the greater amount of organic-carbon per gram in the kerogen versus the whole-rock, as the kerogen contains approximately 6 times the amount of organic carbon per gram than the whole-rock shale. The greater amount of organic carbon in the kerogen probably means there is a greater amount of organic micro-porosity in the kerogen versus the whole-rock, so it is likely that the kerogen has a greater internal surface area available for organic/organic interaction (Ross and Bustin, 2009; Zhang et al., 2012). The different particle size of the adsorbents was not considered to have an influence on the measured chromatographic retention times for hydrocarbons on both adsorbents, as the carrier gas flow rate was held constant at 60 mL/min for both adsorbents; subsequently the calculated ΔH_a values can be considered to be a result of organic/organic interactions only.

6.4.2. Effect of thermal maturity on the surface structure of kerogen

Although it was not a focus of this research, the effect of thermal maturity on the kerogen structure, and subsequently the magnitude of organic/organic interactions, is worth mentioning.

The ΔH_a values measured in this study for the interaction of the same gases with the Green River kerogen and the whole rock shale are very low; it is proposed that these low values are due to the immature nature of the Green River kerogen. Rybolt et al. (2006) and Rybolt et al. (2008) measured ΔH_a values for the interaction of light hydrocarbons with micro-porous and non-porous carbon powders (**Table 5**).

Table 5. Heats of adsorption for the interaction of hydrocarbons with carbon powders, previously determined using the chromatographic method by (a) Rybolt et al. (2006) and (b) Rybolt et al. (2008).

	Adsorbent	Adsorbate	ΔH_a (kcal/mol)
(a)	Carbon powder (nano-porous)	Ethane	- 8.2
		Propane	- 11.5
		n-Butane	- 16.1
		i-Butane	- 15.6
(b)	Carbon powder (non-porous)	i-Butane	- 8.3

Carbon powder adsorbents are proposed to be compositionally similar to over-mature kerogen, as both likely have an aromatic cyclic structure (Vandenbroucke et al.,

2007; Harris et al., 2008). The ring-like structure of the carbon powders and over-mature kerogen make the surfaces of these materials very smooth and planar. Immature kerogen is composed of a mixture of aromatic and aliphatic macromolecules; the aliphatic components make the surface of immature kerogen heterogeneous and rough. As the kerogen matures, H/C and O/C ratios decrease and the kerogen structure becomes increasingly more aromatic (see **Figure 6.2**). The surface heterogeneity of immature kerogen likely increases the distance between the surface and interacting hydrocarbon molecules, effectively decreasing the magnitude of surface/molecule interactions. For the carbon power/over-mature kerogen, the homogenous smooth surface of these adsorbents decreases the distance between the surface and interacting hydrocarbon molecules, effectively increasing the magnitude of the surface/molecule interactions. The structural and elemental differences between these two adsorbents likely contribute to the magnitude of the differences seen between the heats of adsorption for the interaction of hydrocarbons with these adsorbents. The ΔH_a values measured by Rybolt et al. (2006) for the interaction of i-C4 and n-C4 with a carbon powder adsorbent show that i-C4 interacts less with the carbon powder than does n-C4; these data support the conclusion that the stereochemistry of the interacting hydrocarbon molecules affects the magnitude of interaction forces.

The difference between the ΔH_a values measured by Rybolt et al. (2006) and Rybolt et al. (2008) for the interaction of i-C4 with nano-porous and non-porous carbon adsorbents can be attributed to the porosity differences between the two adsorbents. The reasoning behind this is discussed in the following section.

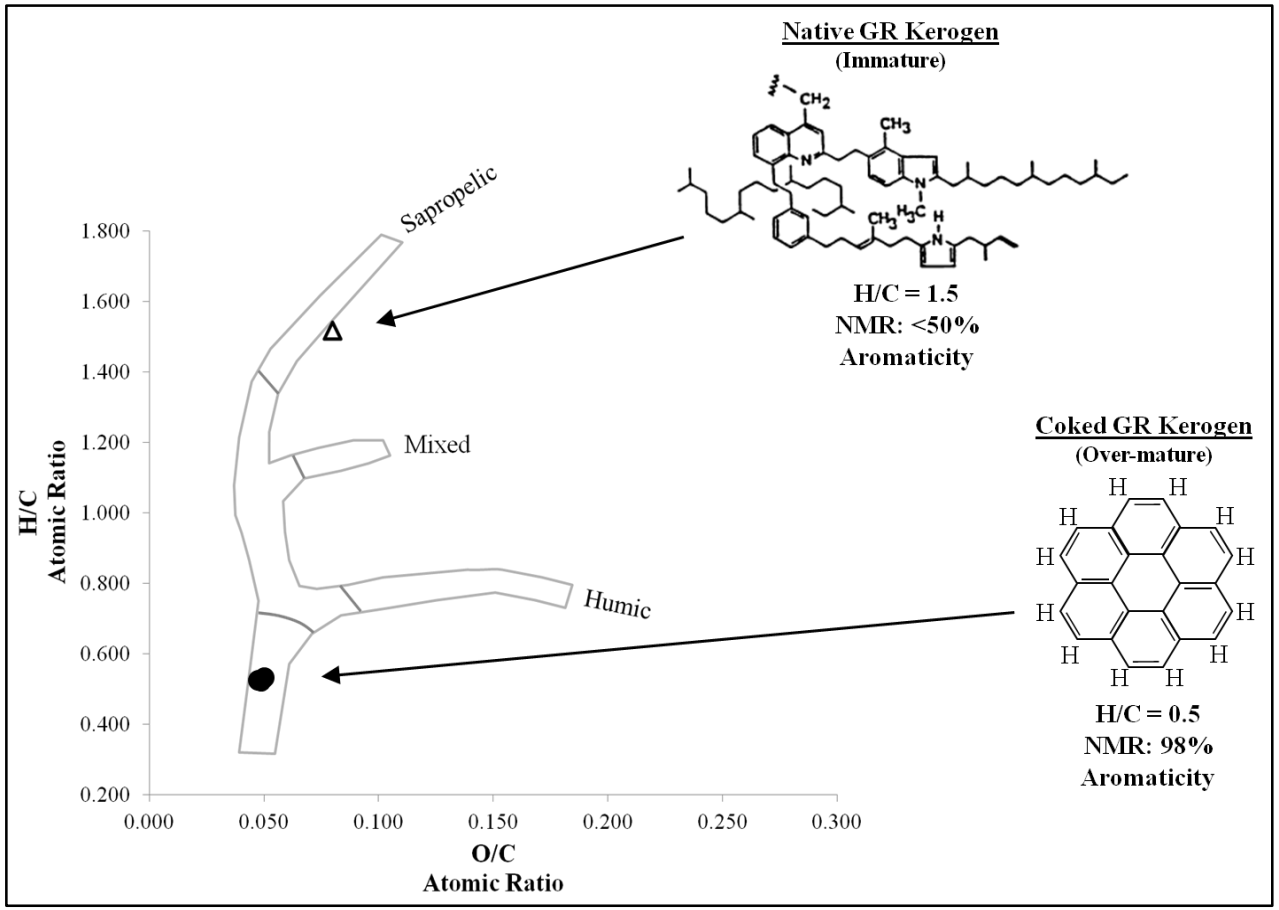

Figure 6.2. Van Krevelen diagram with H/C and O/C ratios plotted for the studied immature Green River kerogen versus a over-mature Green River coke sample. The hypothetical kerogen structures and relative aromaticities are shown for each (Immature kerogen structure modified from Vandenbroucke and Largeau, 2007; aromaticity values for each kerogen, and the relative H/C ratio of the coked samples via personal communications with Dr. K.K. Bissada.

6.4.3. Effect of thermal maturity on organic porosity

Kerogen has a significant amount of micro-porosity in which hydrocarbons can be stored, with the amount of kerogen micro-porosity (and subsequently surface area available for organic/organic interactions) a function of kerogen type and level of thermal maturity; the overall micro-porosity of organic-rich shales increases as the kerogen is converted to hydrocarbon fluids at higher temperatures (Crosdale et al., 1997; Zhang et al., 2012; Rexer et al., 2013). Jarvie et al. (2007) suggest that for thermally mature shales, as much as 4% of the total porosity volume can be attributed to kerogen decomposition. Thus, a source rock at a high level of thermal maturity will have more organic-sourced porosity, and subsequently a greater internal surface area, than would the same source rock at a lower level of thermal maturity. In source rocks with relatively low thermal maturities, such as the studied Green River shale, the kerogen has not yet developed significant thermally-induced micro-porosity. Underdeveloped micro-porosity in the shale kerogen will limit the ability of the whole-rock to adsorb hydrocarbons. Based on this reasoning, it can be assumed that a thermally mature source rock would have a greater internal surface area available for hydrocarbon/surface interaction than the studied thermally immature Green River shale, and measured interaction energies would be greater as a result.

It is difficult to make a direct correlation between the thermal maturity of a source rock and the volume of retained hydrocarbons, as the degree of hydrocarbon retention in organic-rich reservoirs also depends on the composition of the stored hydrocarbon fluids. At high levels of thermal maturity, heavy liquid hydrocarbons will be broken down into

lighter components, which are retained much less readily than the long-chain molecules. So, a thermally mature source rock that has generated both gas and liquid hydrocarbons might have a larger fraction of retained hydrocarbons than a thermally over-mature source rock. More research should be done to constrain the relationship between thermal maturity, kerogen structure, hydrocarbon composition, and the degree of hydrocarbon retention in organic-rich shales.

Chapter 7: Conclusions

The main conclusions established from this study are as follows:

(1) The interaction between light hydrocarbon gases and the examined organic-rich shale is controlled principally by molecule/kerogen dispersion forces. There are no site-specific centers of charge involved and the mineral matrix appears to have no effect on the hydrocarbon adsorption behavior.
(2) Hydrocarbon retention is controlled by the interaction of the two organic structures (hydrocarbon/kerogen). Interaction energies are a function of hydrocarbon molecular size and the distance between the kerogen and the center of mass of the hydrocarbon molecules.
(3) For the n-alkanes, stereochemistry greatly impacts the interaction behavior.

The result of this research was a greater understanding of the physicochemical interactions that can result in the adsorption of hydrocarbons by organic-rich shales, and subsequently influence the degree of hydrocarbon retention in these shales. In order obtain a more comprehensive understanding of hydrocarbon adsorption behavior on kerogen, a more variable sample-set is needed. By studying the interactions controlling hydrocarbon adsorption on kerogen from multiple source rocks, and at variable levels of thermal maturity, information may be gained that can assist in the generation of models of hydrocarbon retention in organically diverse shale plays. These types of models could be used to provide play-specific resource volume estimates, as well as improve current methods used to identify gas-rich zones in organic-rich reservoirs.

Chapter 8: Recommendations

More research must be done to better understand how kerogen composition and level of thermal evolution can affect the hydrocarbon adsorption potential of gas-shales. Suggested avenues of research are as follows:

(1) It should be determined if variable kerogen content influences kerogen/hydrocarbon interactions in organic-rich shales. This could be done by measuring ΔH_a values for the interaction of hydrocarbons on adsorbent mixtures of kerogen and glass-beads. The ratio of kerogen to glass-beads can be adjusted to see if increased kerogen content will result in an increase of kerogen/hydrocarbon interactions.

(2) The influence that kerogen type has on kerogen/hydrocarbon interactions in organic-rich shales needs to be better understood. This can be done by measuring the ΔH_a values for the interaction of hydrocarbons with kerogen isolated from multiple Type I, Type II, and Type III source-shales.

(3) The effect that thermal maturity has on kerogen/hydrocarbon interactions in organic-rich shales should be further investigated. This can be done by measuring and comparing ΔH_a values for the interaction of light-end gas hydrocarbons with an immature kerogen that has been pyrolyzed to various levels of thermal maturity. The structure of the kerogen at each level of maturity could be assessed via focused ion beam scanning electron microscopy (FIB-SEM) and nuclear magnetic resonance (NMR) spectroscopy.

(4) Due to the low thermal maturity of the Green River shale, conditioning the Green River kerogen column at 90°C may have altered the structure of the kerogen; the effect of the column-conditioning on the structure of the kerogen should be determined. This can

be done by using NMR spectroscopy to determine the structure of an unconditioned Green River kerogen versus the structure of the conditioned Green River kerogen used as an adsorbent in the current study. Any structural differences between the two samples would suggest that the column conditioning had an effect on the structure of the kerogen.

(5) An experiment is suggested to determine if carbon powder adsorbents (such as Carbosieve) can be considered analogues to over-mature Green River kerogen. Elemental analysis and NMR spectroscopy could be used to compare the elemental composition and molecular structure of carbon power adsorbents versus a coked Green River kerogen.

References

Adamson, A.W., 1982. *Physical Chemistry of Surfaces*, John Wiley & Sons, New York, 664 p.

Aranovich, G.L., Donohue, M.D., 1995. "Adsorption isotherms for microporous adsorbents", *Carbon,* Vol. 33, pp. 1369 – 1375.

Baker, J. L., 2005. "Geologic and geochemical controls on the generation and accumulation of coalbed methane in southeastern Sandwash Basin, Colorado", M.S. Thesis, University of Houston, 91 p.

Barone, V., Casarin, M., Forrer, D., Pavone, M., Sambi, M., Vittadini, A., 2008. "Role and effective treatment of dispersive forces in materials: polyethylene and graphite crystals as test cases", *Journal of Computational Chemistry*, Vol. 30, pp. 934 – 939.

Bissada, K.K., 1968. "Cation-dipole interactions in clay organic complexes", PhD Dissertation, Washington University, 89 p.

Bissada, K.K., and Johns, W.D., 1969. "Montmorillonite-organic complexes – gas chromatographic determination of energies of interactions", *Clay and Minerals*, Vol. 17, pp. 197 – 204.

Crosdale, P.J., Beamish, B.B., Valix, M., 1998. "Coalbed methane sorption related to coal composition", *International Journal of Coal Geology,* Vol. 35, pp. 147 – 158.

Dal Nogare, S., Juvet, S.J. Jr., 1962. *Gas-Liquid Chromatography: Theory and Practice*, John Wiley & Sons, New York, 450 p.

Demaison, G.J., Moore, G.T., 1980. "Anoxic environments and oil source bed genesis", *The AAPG Bulletin*, Vol. 64, pp. 1179 – 1209.

Dinnebier, R.E., Billinge, S.J.L. (Eds.), 2008. *Powder Diffraction – Theory and Practice*, The Royal Society of Chemistry, Cambridge, 582 p.

Durand, B. (Ed.), 1980. *Kerogen, Insoluble Organic Matter from Sedimentary Rocks*, Éditions Technip, Paris, France, 525 p.

Durand, B., Espitalié, J., 1973. “Evolution de la matiere organique au cours de l’enfouissement des sediments”, *Compte rendus de l’Academeie des Sciences, Paris*, Vol. 276, pp. 2253 – 2256.

Durand, B., Nicaise, G., 1980. “Procedures of kerogen isolation”, in Durand, B. (Ed.), *Kerogen, Insoluble Organic Matter from Sedimentary Rocks*, Éditions Technip, Paris, France, pp. 35 – 53.

EIA, 2011. “Table 4.1 – Technically recoverable crude oil and natural gas resource estimates, 2009”, in U.S. Energy Information Adminstration, *Annual Energy Review 2011*, p. 89. http://www.eia.gov/totalenergy/data/annual/pdf/sec4_3.pdf.

Forsman, J.P., and Hunt, J.M., 1958. “Insoluble organic matter (kerogen) in sedimentary rocks”, *Geochimica et Cosmochimica Acta*, Vol. 15, pp. 170 – 182.

Gregg, S.J., Sing, K.S.W., 1991. *Adsorption, Surface Area, and Porosity*, Academic Press, Waltham, MA, 303 p.

Haar, L., Gallagher, J.S., Kell, G.S., 1984. *NBS/NRC Steam Tables*, Hemisphere Publishing Corp., New York.

Harris, P.J.F., Liu, Z., Suenaga, K., 2008. “Imaging the atomic structure of activated carbon”, *Journal of Physics: Condensed Matter*, Vol. 20, pp. 1 – 5.

Himeno, S., Komatsu, T., Fujita, S., 2005. “High-pressure adsorption equilibria of methane and carbon dioxide on several activated carbons”, *Journal of Chemical and Engineering Data*, Vol. 50, pp. 369 – 376.

Ibrahimov, R.A., and Bissada, K.K., 2010. “Comparative analysis and geological significance of kerogen isolated using open-system (palynological) versus chemically and volumetrically conservative closed-system methods”, *Organic Chemistry*, Vol. 41, pp. 800 – 811.

Jarvie, D.M., Hill, R.J., Ruble, T.E., Pollastro, R.M., 2007. “Unconventional shale-gas systems: the Mississippian Barnett Shale of north-central Texas as one model for thermogenic shale-gas assessment”, *The AAPG Bulletin*, Vol. 91, pp. 475 – 499.

Jenkins, C.D., Boyer, C.M. II., 2008. “Coalbed- and shale-gas reservoirs”, *SPE Journal of Petroleum Technology*, Paper SPE 103514, February 2008, pp. 92 – 99.

Kiselev, A.V., 1965. “Non-specific and specific interactions of molecules of different electronic structures with solid surfaces”, *Discussions of the Faraday Society*, Vol. 40, pp. 205 – 218.

Langmuir, I., 1940. “Monolayers on solids”, Seventeenth Faraday Lecture, *Journal of the American Chemical Society*, pp. 511 – 543.

Ligner, G., Sidqi, M., Jagiello, J., Balard, H., Papirer, E., “Characterization of specific interactions capacity of solid surfaces by adsorption of alkanes and alkenes. Part II: Adsorption on crystalline silica layer surfaces”, *Chromatographia*, Vol. 29, pp. 35 – 38.

London, F., 1930. “Über einige eigenschaften und anwendungen der molekularkräfte”, *Zeitschrift für Physikalische Chemie*, Series B, Vol. 11, pp. 222 – 251.

Muller, P., 1994. “Glossary of terms used in physical organic chemistry – IUPAC Recommendations 1994”, *Pure and Applied Chemistry*, Vol. 66, pp. 1077 – 1184.

Myers, A.L., 2004. “Thermodynamics of adsorption”, in Letcher, T.M., Koukkari, P. (Eds.), *Chemical Thermodynamics for Industry*, Royal Society of Chemistry, Cambridge, Great Britain, pp. 243 – 253.

Qiu, N., Xue, Y., Guo, Y., Sun, W., Chu, W., 2012. “Adsorption of methane on carbon models of coal surface studied by the density functional theory including dispersion correction (DFT-D3)”, *Computational and Theoretical Chemistry*, Vol. 992, pp. 37 – 47.

Rexer, T.F.T., Benham, M.J., Aplin, A.C., Thomas, K.M., 2013. “Methane adsorption on shale under simulated geological temperature and pressure conditions”, *Energy and Fuels*, Vol. 27, pp. 3099 – 3109.

Rigo, V.A., Metin, C.O., Nguyen, Q.P., Miranda, C.R., 2012. “Hydrocarbon adsorption on carbonate mineral surfaces: a first-principles study with van der Waals interactions”, *Journal of Physical Chemistry C*, Vol. 116, pp. 24538 – 24548.

Robinson, W.E., 1969. “Kerogen of the Green River Formation”, in Eglinton, G., Murphy, M.T.J. (Eds.), *Organic Geochemistry – Methods and Results*, Springer Berlin Heidelberg, New York, pp. 619 – 637.

Ross, D.J.K., Bustin, R.M., 2009. “The importance of shale composition and pore structure upon gas storage potential of shale gas reservoirs”, *Marine and Petroleum Geology*, Vol. 26, pp. 916 – 927.

Ross, S., Saelens, J.K., Olivier, J.P., 1962. "On physical adsorption. XVIII. Limiting isosteric heats of adsorption of gases on graphitized carbon by the chromatographic method", *Journal of Physical Chemistry*, Vol. 66, pp. 696 – 700.

Rouquerol, F., Rouquerol, J., Sing, K., 1999. *Adsorption by Powders and Porous Solids – Principles, Methodology and Applications*, Academic Press, London, 465 p.

Rybolt, T.R., Ziegler, K.A., Thomas, H.E., Boyd, J.L., Ridgeway, M.E., 2006. "Adsorption energies for a nanoporous carbon from gas-solid chromatography and molecular mechanics", *Journal of Colloid and Interface Science*, Vol. 296, pp. 41 – 50.

Rybolt, T.R., Wells, C.E., Thomas, H.E., Goodwin, C.M, Blakely, J.L., Turner, J.D., 2008. "Binding energies for alkane molecules on a carbon surface from gas-solid chromatography and molecular mechanics", *Journal of Colloid and Interface Science*, Vol. 325, pp. 282 – 286.

Saxby, J.D., 1970. "Isolation of kerogen in sediments by chemical methods", *Chemical Geology*, Vol. 6, pp. 173 – 184.

Schenk, C.J., Pollastro, R.M., 2002. "Natural gas production in the United States: national assessment of oil and gas series, 2002", *U.S. Geological Survey Fact Sheet FS-113-01*, pp. 1 – 2.

Seewald, J.S., Benitez-Nelson, B.C., Whelan, J.K., 1998. "Laboratory and theoretical constraints on the generation and composition of natural gas", *Geochimica et Cosmochimica Acta*, Vol. 62, pp. 1599 – 1617.

Sondergeld, C.H., Newsham, K.E., Comisky, J.T., Rice, M.C., Rai, C.S., 2010. "Petrophysical considerations in evaluating and producing shale gas resources", *SPE Unconventional Gas Conference*, Paper SPE 131768, February 2010, pp. 1 – 34.

Speight, J.G., 2013. *Shale Gas Production Processes*, Elsevier, 162 p.

Stainforth, J.G., Reinders, J.E.A., 1990. "Primary migration of hydrocarbons by diffusion through organic matter networks, and its effect on oil and gas generation", *Advances in Organic Geochemistry 1989*, Vol. 16, pp. 61 – 74.

Thomas, M.M., Clouse, J.A., 1990a. "Primary migration by diffusion through kerogen: I. Model experiments with organic-coated rocks", *Geochimica et Cosmochimica Acta*, Vol. 54, pp. 2775 – 2779.

Thomas, M.M., Clouse, J.A., 1990b. “Primary migration by diffusion through kerogen: II. Hydrocarbon diffusivities in kerogen”, *Geochimica et Cosmochimica Acta*, Vol. 54, pp. 2781 – 2792.

Tissot, B., Durand, B., Espitalié, J., Combaz, A., 1974. “Influence of nature and diagenesis of organic matter in formation of petroleum”, *The AAPG Bulletin*, Vol. 58, pp. 499 – 506.

Tissot, B., Welte, D.H., 1978. *Petroleum Formation and Occurrence: A New Approach to Oil and Gas Exploration*, Springer-Verlag Berlin, Heidelberg, Germany, 147 p.

USGS National Assessment of Oil and Gas Resources Team, and Biewick, L.R.H., compiler, 2013a. “Map of assessed shale gas in the United States, 2012”, in *U.S. Geological Survey Digital Data Series 69–Z*, pp. 1-16.

USGS National Assessment of Oil and Gas Resources Team, 2013b. “Continuous Gas Resources”, in *U.S. Geological Survey National Assessment of Oil and Gas Resources Update*, March 2013, *http://certmapper.cr.usgs.gov/data/noga00/natl/tabular/2013/Summary_13_Cont_Gas.pdf*

USGS National Assessment of Oil and Gas Resources Team, and Biewick, L.R.H., compiler, 2014. “Map of assessed tight-gas resources in the United States, 2014”, in *U.S. Geological Survey Digital Data Series 69–HH*, 6 p., 1 pl., GIS data package, *http://dx.doi.org/10.3133/ds69HH*.

Vanden Berg, M.D., 2008. “Basin-wide evaluation of the uppermost Green River formation’s oil-shale resource, Uinta Basin, Utah and Colorado”, *Special Study 128*, Utah Geological Survey, Salt Lake City, Utah, pp. 1 – 19.

Vandenbroucke, M., Largeau, C., 2007. “Kerogen origin, evolution and structure”, *Organic Geochemistry*, Vol. 38, pp. 719 – 833.

Xia, X., Tang, Y., 2012. “Isotope fractionation of methane during natural gas flow with coupled diffusion and adsorption/desorption”, *Geochimica et Cosmochimica Acta*, Vol. 77, pp. 489 – 503.

Yang, C., Huang, W., Fu, J., Dang, Z., 2009. “Impact of kerogen heterogeneity on sorption of organic pollutants. 1. Sorbent characterization”, *Environmental Toxicology and Chemistry*, Vol. 28, pp. 1585 – 1591.

Zhang, T., Ellis, G.S., Ruppel, S.C., Milliken, K., Yang, R., 2012. “Effect of organic-matter type and thermal maturity on methane adsorption in shale-gas systems”, *Organic Geochemistry*, Vol. 47, pp. 120 – 131.